BRARY
AVAL POSTGRADUATE SCHOOL
ONTEREY, CALIFORNIA 93940

NSWC-TR-89-180

WIND TUNNEL TESTS OF A 20-GORE DISK-GAP-BAND PARACHUTE

ADA 221 326

BY WILLIAM P. LUDTKE

UNDERWATER SYSTEMS DEPARTMENT

28 MAY 1989

Approved for public release; distribution is unlimited.

Change 1 inserted.

NAVAL SURFACE WARFARE CENTER

Dahlgren, Virginia 22448-5000 • Silver Spring, Maryland 20903-5000

DEPARTMENT OF THE NAVY
NAVAL SURFACE WARFARE CENTER
DAHLGREN, VIRGINIA 22448-5000

WHITE OAK
10901 NEW HAMPSHIRE AVE.
SILVER SPRING, MD. 20903-5000
(202) 394- 4404
DAHLGREN, VA. 22448-5000
(703) 663-

IN REPLY REFER TO:
E221:MEM

Change 1
2 Jul 90

U245669

To all holders of NSWC TR 89-180
Title: Wind Tunnel Tests of a 20-Gore Disk-Gap-Band Parachute

3 page (s)

This publication is changed as follows:

Remove the following pages and replace with new pages supplied:

34-35

Done 8/23/90 [illegible]

Insert this change sheet between the cover and the DD Form 1473 in your copy.
Write on the cover "Change 1 inserted"

Approved by:

J. E. Goeller

J. E. GOELLER, Deputy Head
Underwater Systems Department

REPORT DOCUMENTATION PAGE

1a. REPORT SECURITY CLASSIFICATION UNCLASSIFIED	1b. RESTRICTIVE MARKINGS
2a. SECURITY CLASSIFICATION AUTHORITY	3. DISTRIBUTION/AVAILABILITY OF REPORT Approved for public release; distribution is unlimited.
2b. DECLASSIFICATION/DOWNGRADING SCHEDULE	
4. PERFORMING ORGANIZATION REPORT NUMBER(S) NSWC TR 89-180	5. MONITORING ORGANIZATION REPORT NUMBER(S)
6a. NAME OF PERFORMING ORGANIZATION Naval Surface Warfare Center 6b. OFFICE SYMBOL (If applicable) U13	7a. NAME OF MONITORING ORGANIZATION
6c. ADDRESS (City, State, and ZIP Code) 10901 New Hampshire Avenue Silver Spring, MD 20903-5000	7b. ADDRESS (City, State, and ZIP Code)
8a. NAME OF FUNDING/SPONSORING ORGANIZATION 8b. OFFICE SYMBOL (If applicable)	9. PROCUREMENT INSTRUMENT IDENTIFICATION NUMBER
8c. ADDRESS (City, State, and ZIP Code)	10. SOURCE OF FUNDING NOS. PROGRAM ELEMENT NO.: NA PROJECT NO.: 9U81VB TASK NO.: NA WORK UNIT NO.: NA
11. TITLE (Include Security Classification) Wind Tunnel Tests of a 20-Gore Disk-Gap-Band Parachute	
12. PERSONAL AUTHOR(S) William P. Ludtke	
13a. TYPE OF REPORT Final 13b. TIME COVERED FROM FY89 TO FY90	14. DATE OF REPORT (Yr., Mo., Day) 1989 May 28 15. PAGE COUNT
16. SUPPLEMENTARY NOTATION	

17. COSATI CODES		
FIELD	GROUP	SUB. GR.
01	03	

18. SUBJECT TERMS (Continue on reverse if necessary and identify by block number)

Disk-Gap-Band Parachutes
Parachute Technology
Opening Shock
Stability
Design Data
Effects of Geometry on Aerodynamic Properties

19. ABSTRACT (Continue on reverse if necessary and identify by block number)

This report documents wind tunnel tests of a series of 20 gore Disk-Gap-Band parachutes to determine the effects off gap length, band length, band billow, and cloth air permeability on the parachute aerodynamic characteristics. Measurements for the steady-state drag-force, opening shock force, oscillation stability, and inflation stability were made of the various configurations and are presented in tabular and graphical format.

20. DISTRIBUTION/AVAILABILITY OF ABSTRACT X UNCLASSIFIED/UNLIMITED ___ SAME AS RPT ___ DTIC USERS	21. ABSTRACT SECURITY CLASSIFICATION UNCLASSIFIED
22a. NAME OF RESPONSIBLE INDIVIDUAL Willaim P. Ludtke	22b. TELEPHONE NUMBER (Include Area Code) (202) 394-1705 22c. OFFICE SYMBOL U13

DD FORM 1473, 84 MAR 83 APR edition may be used until exhausted
All other editions are obsolete

UNCLASSIFIED
SECURITY CLASSIFICATION OF THIS PAGE

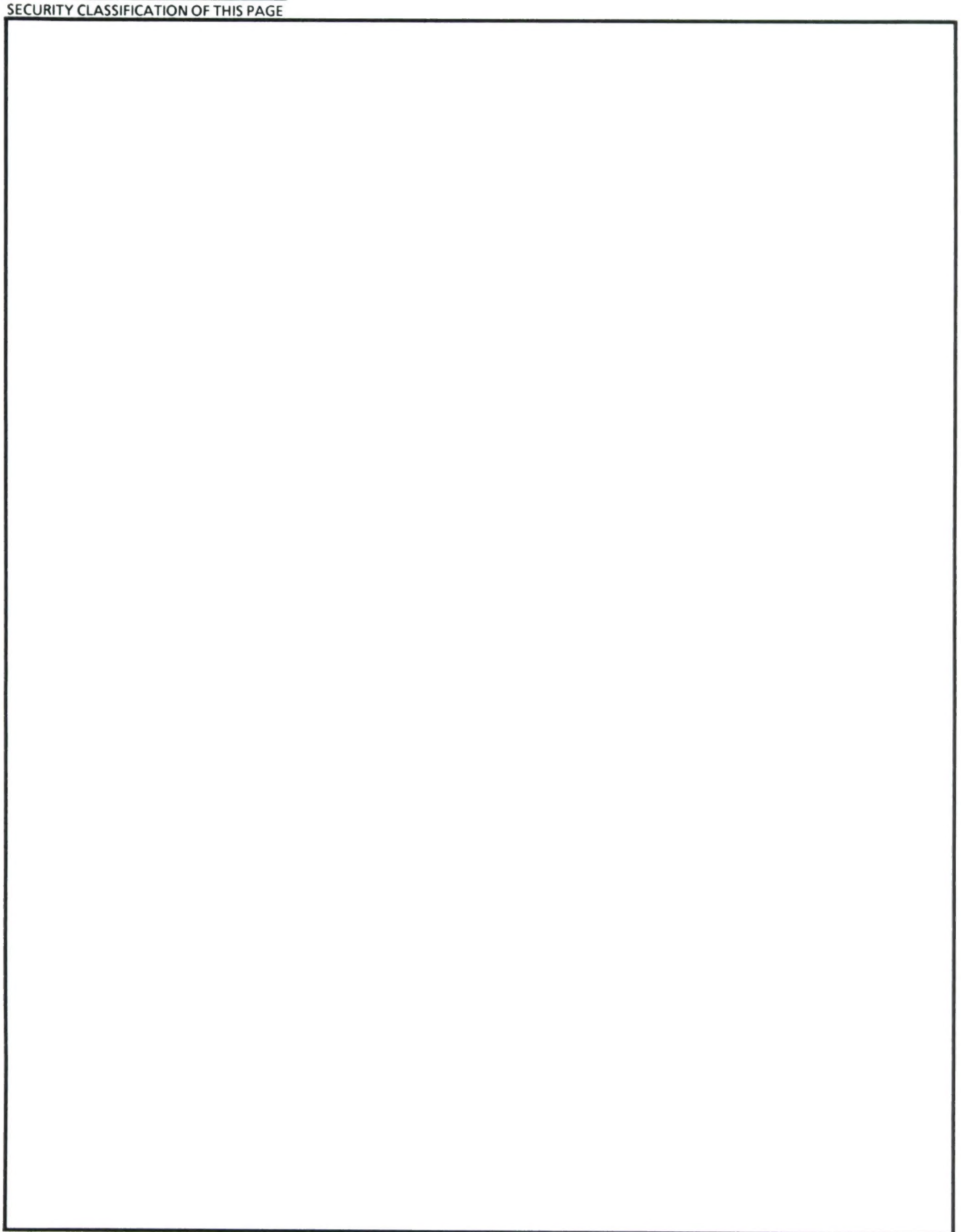

FOREWORD

This report documents wind tunnel tests of a series of 20 gore Disk-Gap-Band parachutes to determine the effects of gap length, band length band billow, and cloth air permeability on the parachute aerodynamic characteristics. Measurements for the steady-state drag force, opening shock force, oscillation stability, and inflation stability were made of the various configurations and are presented in tabular and graphical format.

Approved by:

W. W. Wassmann

W. W. WASSMANN, Head
Underwater Weapons Division

CONTENTS

	Page
INTRODUCTION	1
SUMMARY	3
MODEL PARACHUTES	5
TEST METHOD	9
DATA REDUCTION	11
TEST RESULTS	25
OPENING SHOCK FACTOR	35
DISCUSSION	43
CONCLUSIONS	45
NOMENCLATURE	47
REFERENCES	49

ILLUSTRATIONS

Figure		Page
1	20 GORE DISK-GAP-BAND PARACHUTE MODEL	6
2	EFFECTS OF GAP LENGTH AND BAND LENGTH ON THE PARACHUTE DRAG AREA FOR VARIOUS BAND BILLOW ALLOWANCES	26
3	EFFECTS OF CLOTH PERMEABILITY, GAP LENGTH, AND BAND BILLOW ON THE DISK-GAP-BAND PARACHUTE DRAG AREA FOR L_B = 8 INCHES, L_B/D_o = 0.2491	29
4	PHOTOGRAPHS OF STEADY-STATE INFLATED PARACHUTE CANOPIES WITH A BAND LENGTH OF 4 INCHES.	31
5	COMPARISON OF THE OSCILLATIONS OF THE SOLID CLOTH FLAT CIRCULAR AND DISK-GAP-BAND PARACHUTES AT 150 MPH	33
6	EFFECTS OF CLOTH PERMEABILITY, GAP LENGTH, AND BAND BILLOW ON THE MAXIMUM OSCILLATION ANGLE OF THE SEVERAL PARACHUTES FOR AN L_B = 8 INCHES	34
7	TYPICAL PARACHUTE OPENING FORCE TEST RECORDS	37
8	EXPANDED OPENING SHOCK SIGNATURES TO DEMONSTRATE LINEARITY OF DRAG AREA DURING INFLATION	39
9	AVERAGE SHOCK FACTOR VERSUS CLOTH PERMEABILITY WITH 1 SIGMA VARIATION	41

TABLES

Table		Page
1	MATERIALS USED IN MODEL PARACHUTE CONSTRUCTION	7
2	SUMMARY OF DISK-GAP-BAND PARACHUTE WIND TUNNEL TEST DATA	13
3	SUMMARY OF AVERAGE OPENING SHOCK FACTORS FOR ALL CONFIGURATIONS L_B = 8 INCHES, L_B/D_o = 0.2491	40

INTRODUCTION

The purpose of the wind tunnel test was to obtain engineering data for use in the design of Disk-Gap-Band (DGB) parachutes. Twenty-seven model parachutes were constructed to evaluate the effects of cloth permeability, gap length, band length, and band billow width on the infinite mass deployment forces, inflation characteristics, stability, and drag-producing qualities of the DGB design. One hundred twenty-one test runs were conducted to obtain the test data. Due to the limited wind tunnel testing time available, only 20 gore canopies were tested. The number of canopy gores may be another performance variable. Steady-state-drag-force tests were made on all band length and width configurations, but deployment forces were measured only on models with band lengths of 8 inches. The many possible test combinations have provided a large quantity of interrelated performance data.

SUMMARY

The wind tunnel tests have demonstrated that the aerodynamic drag area, stability, opening force, and inflation characteristics of the model parachutes are determined by the rate of airflow through the canopies. Model parachute airflow variation was controlled by the cloth permeability, the length of the gap between the disk and the band, and the cloth area of the parachute band.

The performance of the model parachutes of similar geometric configuration, varied as a result of the canopy airflow control. Low permeability cloth of specification MIL-C-7219 together with a minimum gap length resulted in a fully inflated, high-drag area model that either coned about the center line of the wind tunnel with the parachute center line at a constant shallow angle or coned and oscillated. Identical models made from the higher rate of airflow cloth of specification MIL-C-7020 had improved stability and a reduced drag area distribution. These models did not cone, but oscillated at shallow angles to the wind tunnel center line. The third set of identical models was manufactured using the cloth of specification MIL-C-17208. This highest rate of airflow cloth further reduced the available drag area for the same geometric configurations.

All models with the MIL-C-7219 cloth inflated when deployed during the opening force tests. All models with the MIL-C-7020 cloth inflated when deployed except in one test of model parachute number 31 with a 6-inch-gap length and $W_B = 6\text{-}1/16$ inches. The model did inflate in subsequent tests. Band inflation instability in the steady-state test photographs of Figure 4 can be seen in test run number 110. Model parachutes made from the MIL-C-17208 cloth and numbered 34, 37, and 40 with a gap length of 6 inches and $W_B = 4\text{-}9/16$, 5-1/16, and 6-1/16, respectively, had inflation difficulties. The band of the $W_B = 4\text{-}9/16$ and 6-1/16 models did not inflate while the $W_B = 5\text{-}1/16$-inch design fully inflated once, inflated after a time delay once, and failed to inflate once, see Figure 4, which demonstrates that the boundary of inflation reliability has been achieved.

The forces generated by the inflating parachutes were surprisingly low. Solid-cloth parachutes usually deploy with "infinite mass" shock factors of approximately 1.8 to 2. Maximum inflation force factors of the Disk-Gap-Band parachute are difficult to distinguish from snatch factors developed from accelerations which occur at line stretch. The apparent cause of the low opening force factors is the considerable damping of the inflation process by the yet-to-be inflated band cloth. A detailed discussion of the data is presented under test results. The variation of the dynamic drag area during inflation is linear with deployment time ratio.

MODEL PARACHUTES

All models were constructed as per Figure 1 using the materials listed in Table 1. The geometry of the disk is identical for all models. The band length was initially constructed 12 inches long with provision for modification in 4-inch increments. The circumferential tapes on the band provided similar hem configurations as the models were modified. Model parachutes were constructed with gap length dimensions, G, of 2, 4, and 6 inches and gore billow allowances, W_B, of 4-9/16, 5-1/16, and 6-1/16 inches which represent gore band circumferences of less than, equal to, and greater than the nominal 5-1/16-inch disk gore skirt hem width. An initial suspension line length of 60 inches was selected as representative of an average one parachute diameter length. The parachute diameter includes the length of the two band and gap lengths along with the central disk diameter. Removal of the 4-inch-wide band panels results in a lengthening of the suspension lines.

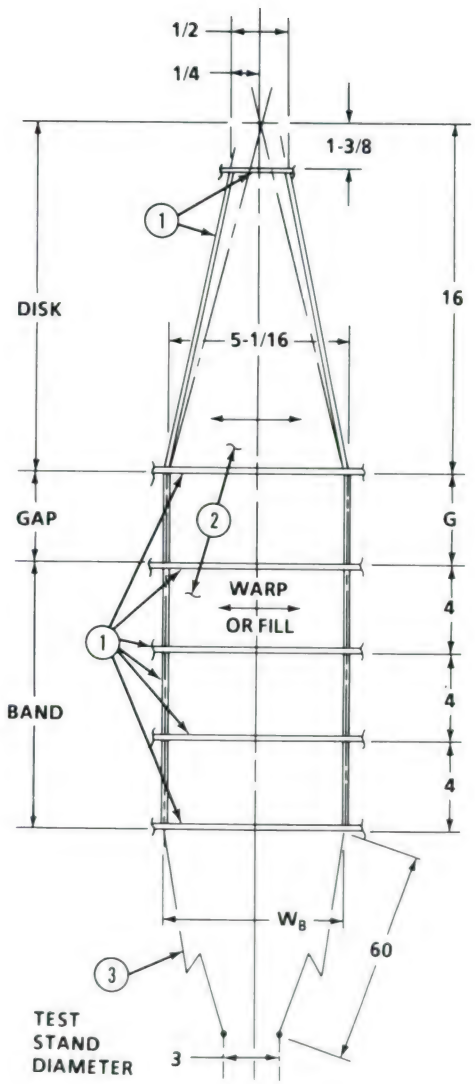

1. TAPE
2. CANOPY CLOTH
3. SUSPENSION LINE

SEE TABLE 1 FOR LIST OF MATERIALS

PARACHUTE REFERENCE AREAS							
	BAND AREA S_B FT^2			DISK AREA S_D FT^2	TOTAL AREA S_T FT^2		
W_B IN \ L_B IN	4	8	12		4	8	12
4-9/16	5.069	2.535	7.604	5.625	8.160	10.694	13.229
5-1/16	5.625	2.812	8.437	5.625	8.437	11.250	14.062
6-1/16	6.736	3.368	10.104	5.625	8.993	12.361	15.729

NORMALIZED CANOPY DIMENSIONS					
GAP		W_B		BAND	
LENGTH INCHES	LENGTH Do	WIDTH INCHES	WIDTH Do	LENGTH INCHES	LENGTH Do
2	0.0623	4-9/16	0.1421	4	0.1246
4	0.1246	5-1/16	0.1576	8	0.2491
6	0.1868	6-1/16	0.1888	12	0.3737

MODEL NO.	PARACHUTE GAP AND BAND DIMENSIONS		
	CLOTH MIL-C-	GAP G INCHES	BAND W_B INCHES
14	7219	2	4-9/16
15		4	4-9/16
16		6	4-9/16
17		2	5-1/16
18		4	5-1/16
19		6	5-1/16
20		2	6-1/16
21		4	6-1/16
22		6	6-1/16
23	7020	2	4-9/16
24		4	4-9/16
25		6	4-9/16
26		2	5-1/16
27		4	5-1/16
28		6	5-1/16
29		2	6-1/16
30		4	6-1/16
31		6	6-1/16
32	17208	2	4-9/16
33		4	4-9/16
34		6	4-9/16
35		2	5-1/16
36		4	5-1/16
37		6	5-1/16
38		2	6-1/16
39		4	6-1/16
40		6	6-1/16

FIGURE 1. 20 GORE DISK GAP BAND PARACHUTE MODEL

TABLE 1. MATERIALS USED IN MODEL PARACHUTE CONSTRUCTION

ITEM	MATERIAL	PARACHUTE MODELS		
		NUMBERS 14 TO 22	NUMBERS 23 TO 31	NUMBERS 32 TO 40
1	CLOTH	MIL-C-7219, TYPE I AIR PERMEABILITY 5.2 CFM/FT^2 @ 1/2 INCH WATER PRESSURE DIFFERENTIAL	MIL-C-7020, TYPE I AIR PERMEABILITY 93.9 CFM/FT^2 @ 1/2 INCH WATER PRESSURE DIFFERENTIAL	MIL-C-17208, TYPE I, CLASS C AIR PERMEABILITY 237.0 CFM/FT^2 @ 1/2 INCH WATER PRESSURE DIFFERENTIAL
2	TAPE	MIL-T-5038 TYPE III, 1/2 INCH WIDE	MIL-T-5038 TYPE III, 1/2 INCH WIDE	MIL-T-5038 TYPE III, 1/2 INCH WIDE
3	SUSPENSION LINE	MIL-C-17183, TYPE III	MIL-C-17183, TYPE III	MIL-C-17183, TYPE III
4	STITCHES[1]	TYPE 301, FED STD 751, 9 TO 12 STITCHES PER INCH, 2 ROWS ON 1/4 INCH NEEDLE GUAGE.		
5	STITCHES	TYPE 301, FED STD 751, 9 TO 12 STITCHES PER INCH, SINGLE ROW		

[1] ALL THREAD, V-T-295. TYPE II, CLASS 1 OR 2, SIZE B

TEST METHOD

The wind tunnel test was conducted at the University of Maryland Wind Tunnel. This facility has a test velocity capability of 200 mph in a test section of 7 feet high, 11 feet wide, and 14 feet long.

An instrumented test stand was installed on the center line of the test section to electronically record the steady-state drag forces or deployment force-time signatures of the various parachute models. The wind tunnel dynamic pressure variation during deployment tests was simultaneously recorded with the deployment force. Steady-state drag areas and deployment maximum load factors were computed by the methods discussed in the test data reduction program and are furnished in the data.

A test sequence consisted of attaching a model parachute's suspension lines to connectors uniformly distributed around the circumference of a 3-inch-diameter-circle. The wind tunnel was accelerated to 200 mph and the steady-state drag force and dynamic pressure were recorded by the instrumentation. When the wind tunnel could be entered, the model was modified by removing the first 4-inch length of the band. The parachute was then packed inside the test stand and a small extraction parachute attached. When the wind tunnel attained 200 mph, the inflated extraction parachute was released and deployed the model from the test stand. After the opening force-time measurements were obtained, the wind tunnel was brought back to 200 miles per hour for steady-state data. Each model was deployed twice. After the deployment tests, the second 4-inch band segment was removed and the steady-state tests repeated. Motion picture and still photographic coverage of selected tests was obtained and are included in the results.

DATA REDUCTION

The test data was reduced by means of the following formulas.

PARACHUTE STEADY-STATE AERODYNAMIC SIZE, FT^2

$$C_D S_O = \frac{F_{SS}}{q_{SS}}$$

DRAG COEFFICIENT REFERENCE AREAS

Disk Area

$$S_D = \frac{NWR}{2 \times 144}$$

$$S_D = \frac{20 \times 5.0625 \times 16}{2 \times 144}$$

$$S_D = 5.625 \text{ ft}^2$$

Band Area

$$S_B = \frac{NW_B L_B}{144}$$

$$S_B = \frac{20 W_B L_B}{144}$$

S_B varies with the band width and length dimensions of the particular model

Total Canopy Area

$$S_T = S_D + S_B$$

The several areas are summarized in Figure 1.

DRAG COEFFICIENTS

Based on disk area

$$C_{DD} = \frac{C_D S_O}{S_D}$$

Based on total area

$$C_{DT} = \frac{C_D S_O}{S_T}$$

Drag coefficients based on disk area and total area are presented in Table 2.

SNATCH FACTOR

As the parachute separates from the test stand, the flow of air accelerates the deploying parachute. Upon reaching line stretch, the mass of the parachute and the entrapped air must be decelerated. This sudden deceleration causes a short duration force to be applied to the system.

After deployment of the canopy, the steady-state drag force is not necessarily recorded at the same dynamic pressure as the snatch force or maximum force. Therefore, the steady-state drag force must be adjusted for the variation from the steady-state conditions.

Adjusted drag force

$$F = F_{SS}\left(\frac{q \text{ @ snatch force}}{q_{SS}}\right)$$

Snatch factor

$$S.F. = \frac{\text{Snatch Force}}{F}$$

TABLE 2. SUMMARY OF DISK-GAP-BAND PARACHUTE WIND TUNNEL TEST DATA

	MODEL DATA						STEADY STATE					DEPLOYMENT					REMARKS
										DRAG COEFFICIENT							
RUN NO.	PARACHUTE MODEL NO.	CANOPY CLOTH MIL-C-	GAP WIDTH G (in)	BAND BILLOW W_B (in)	BAND LENGTH L_B (in)	DEPLOY TEST	F_{SS} (lb)	q_{SS} (psf)	C_DS_O (ft^2)	DISK AREA C_{DD}	TOTAL AREA C_{DT}	MAX FORCE F_{MAX} (lb)	q @F_{MAX} (psf)	C_DS MAX (ft^2)	SHOCK FACTOR K	AVERAGE SHOCK FACTOR K_{av}	
33	14	7219	2	4 9/16	12		655.1	102.83	6.371	1.133	0.482						
34	14	7219	2	4 9/16	8	YES	662.6	97.96	6.764	1.203	0.633	761.5	102.28	7.446	1.101	1.069	
35	14	7219	2	4 9/16	8	YES	672.6	98.01	6.862	1.220	0.642	725.0	101.99	7.059	1.036		
36	14	7219	2	4 9/16	4		639.2	100.40	6.366	1.132	0.634						
38	15	7219	4	4 9/16	12		612.5	101.56	6.031	1.072	0.456						
68	15	7219	4	4 9/16	8	YES	703.0	93.64	7.508	1.335	0.920	875.6	102.84	8.514	1.134	1.134	
39	16	7219	6	4 9/16	12		596.9	102.12	5.845	1.039	0.442						
40	16	7219	6	4 9/16	8	YES	628.7	99.16	6.340	1.127	0.593	809.1	101.77	7.950	1.254	1.409	
41	16	7219	6	4 9/16	8	YES	607.6	97.07	6.260	1.113	0.585	1001.5	102.32	9.788	1.564		
42	16	7219	6	4 9/16	4		592.3	101.06	5.861	1.042	0.718						
44	17	7219	2	5 1/16	12		757.6	97.38	7.780	1.383	0.553						
45	17	7219	2	5 1/16	8	YES	762.6	92.65	8.231	1.463	0.732	941.1	104.67	8.991	1.092	1.092	
46	17	7219	2	5 1/16	8	YES	776.6	93.18	8.334	1.482	0.741	930.8	102.28	9.101	1.092		
48	17	7219	2	5 1/16	4		686.3	97.26	7.057	1.255	0.836						
111	18	7219	4	5 1/16	12		701.0	99.56	7.041	1.252	0.501						
113	18	7219	4	5 1/16	8	YES	729.4	96.41	7.566	1.345	0.673	846.3	101.93	8.303	1.097	1.078	
115	18	7219	4	5 1/16	8	YES	734.4	95.40	7.698	1.368	0.684	829.3	101.80	8.146	1.058		
116	18	7219	4	5 1/16	4		596.2	98.33	6.063	1.078	0.719						
50	19	7219	6	5 1/16	12		648.7	101.20	6.410	1.140	0.456						
51	19	7219	6	5 1/16	8	YES	684.3	97.09	7.048	1.253	0.627	805.1	103.43	7.784	1.104	1.101	
52	19	7219	6	5 1/16	8	YES	683.3	96.96	7.047	1.253	0.626	788.4	101.93	7.735	1.098		
53	19	7219	6	5 1/16	4		643.1	99.97	6.433	1.144	0.768						

TABLE 2. SUMMARY OF DISK-GAP-BAND PARACHUTE WIND TUNNEL TEST DATA (Continued)

	MODEL DATA						STEADY STATE					DEPLOYMENT					REMARKS
										DRAG COEFFICIENT							
RUN NO.	PARACHUTE MODEL NO.	CANOPY CLOTH MIL-C-	GAP WIDTH G (in)	BAND BILLOW W_B (in)	BAND LENGTH L_B (in)	DEPLOY TEST	F_{SS} (lb)	q_{SS} (psf)	C_DS_O (ft^2)	DISK AREA C_{DD}	TOTAL AREA C_{DT}	MAX FORCE F_{MAX} (lb)	q @F_{MAX} (psf)	C_DS MAX (ft^2)	SHOCK FACTOR K	AVERAGE SHOCK FACTOR K_{av}	
55	20	7219	2	6 1/16	12		930.2	88.05	10.564	1.878	0.672						
56	20	7219	2	6 1/16	8	YES	905.5	83.36	10.862	1.952	0.876	1331.1	110.31	12.067	1.111	1.043	
57	20	7219	2	6 1/16	8	YES	908.4	83.98	10.818	1.923	0.875	1258.8	119.21	10.559	0.976		
58	20	7219	2	6 1/16	8		717.3	95.74	7.492	1.332	0.833						
59	20	7219	2	6 1/16	4		725.4	95.16	7.623	1.355	0.848						
60	21	7219	4	6 1/16	12		869.9	90.51	9.611	1.709	0.611						
61	21	7219	4	6 1/16	8	YES	869.3	87.15	9.975	1.773	0.804	1401.8	102.45	13.683	1.372	1.157	
62	21	7219	4	6 1/16	8	YES	885.2	87.21	10.151	1.805	0821	1024.1	107.24	9.550	0.941		
63	21	7219	4	6 1/16	4		674.2	96.71	6.972	1.240	0.775						
64	22	7219	6	6 1/16	12		768.8	92.63	8.299	1.475	0.528						
65	22	7219	6	6 1/16	8	YES	778.5	88.98	8.750	1.556	0.708	1004.5	102.38	9.811	1.121	1.105	
66	22	7219	6	6 1/16	8	YES	839.3	88.04	9.533	1.556	0.771	1115.0	107.39	10.382	1.089		
67	22	7219	6	6 1/16	4		621.9	96.36	6.455	1.148	0.718						
69	23	7020	2	4 9/16	12		575.4	102.06	5.638	1.002	0.426						
70	23	7020	2	4 9/16	8	YES	570.9	98.98	5.768	1.025	0.539	678.9	101.12	6.714	1.164		
71	23	7020	2	4 9/16	8	YES	535.5	83.66	6.402	1.138	0.599	612.8	102.69	5.968	0.932	1.048	
72	23	7020	2	4 9/16	4		548.9	101.21	5.423	0.964	0.665						
74	24	7020	4	4 9/16	12		504.8	102.37	4.932	0.877	0.373						
75	24	7020	4	4 9/16	8	YES	596.9	101.86	5.860	1.042	0.548	678.4	102.28	6.634	1.132		
76	24	7020	4	4 9/16	8	YES	565.0	100.00	5.651	1.005	0.528	588.9	100.69	5.849	1.035	1.083	
77	24	7020	4	4 9/16	8		608.0	99.68	6.099	1.084	0.570						

TABLE 2. SUMMARY OF DISK-GAP-BAND PARACHUTE WIND TUNNEL TEST DATA (Continued)

	MODEL DATA						STEADY STATE					DEPLOYMENT					REMARKS
										DRAG COEFFICIENT							
RUN NO.	PARACHUTE MODEL NO.	CANOPY CLOTH MIL-C-	GAP WIDTH G (in)	BAND BILLOW W_B (in)	BAND LENGTH L_B (in)	DEPLOY TEST	F_{SS} (lb)	q_{SS} (psf)	C_DS_O (ft^2)	DISK AREA C_{DD}	TOTAL AREA C_{DT}	MAX FORCE F_{MAX} (lb)	q @F_{MAX} (psf)	C_DS MAX (ft^2)	SHOCK FACTOR K	AVERAGE SHOCK FACTOR K_{av}	
78	24	7020	4	4 9/16	4		509.7	102.13	4.991	0.887	0.612						
79	25	7020	6	4 9/16	12		508.7	102.18	4.978	0.885	0.376						
80	25	7020	6	4 9/16	8	YES	579.8	100.55	5.766	1.025	0.539	631.2	101.97	6.190	1.073	1.063	
81	25	7020	6	4 9/16	8	YES	546.7	100.23	5.455	0.970	0.510	576.2	102.04	5.647	1.054		
82	25	7020	6	4 9/16	4		558.6	102.69	5.439	0.967	0.667						
83	26	7020	2	5 1/16	12		670.3	97.45	6.878	1.223	0.489						
84	26	7020	2	5 1/16	8	YES	697.2	94.46	7.381	1.312	0.656	946.7	102.10	9.272	1.256	1.149	
85	26	7020	2	5 1/16	8	YES	629.5	94.22	6.681	1.188	0.594	710.0	101.99	6.961	1.042		
86	26	7020	2	5 1/16	4		599.7	99.41	6.033	1.073	0.715						
87	27	7020	4	5 1/16	12		634.3	99.05	6.404	1.138	0.455						
88	27	7020	4	5 1/16	8	YES	629.1	96.03	6.551	1.165	0.582	662.7	102.21	6.484	0.990	1.019	
89	27	7020	4	5 1/16	8	YES	615.3	96.32	6.388	1.136	0.568	643.5	96.05	6.700	1.049		
90	27	7020	4	5 1/16	4		566.3	100.53	5.633	1.001	0.668						
91	28	7020	6	5 1/16	12		556.2	98.14	5.667	1.008	0.403						
92	28	7020	6	5 1/16	8	YES	581.3	97.09	5.987	1.064	0.532	671.1	102.19	6.567	1.097	1.132	
93	28	7020	6	5 1/16	8	YES	530.3	96.74	5.482	0.975	0.487	653.5	102.25	6.391	1.166		
94	28	7020	6	5 1/16	4		568.1	101.14	5.617	0.999	0.666						
95	29	7020	2	6 1/16	12		812.6	87.50	9.286	1.651	0.590						
96	29	7020	2	6 1/16	8	YES	795.0	86.39	9.203	1.636	0.745	954.1	102.54	9.305	1.011		
97	29	7020	2	6 1/16	8	YES	798.4	86.74	9.205	1.636	0.745					0.998	
98	29	7020	2	6 1/16	8	YES	741.0	86.28	8.589	1.527	0.695	862.1	101.88	8.462	0.985		
99	29	7020	2	6 1/16	4		649.8	98.62	6.590	1.172	0.733						
100	30	7020	4	6 1/16	12		764.0	90.16	8.471	1.507	0.539						

TABLE 2. SUMMARY OF DISK-GAP-BAND PARACHUTE WIND TUNNEL TEST DATA (Continued)

TABLE 2. SUMMARY OF DISK-GAP-BAND PARACHUTE WIND TUNNEL TEST DATA (Continued)

	MODEL DATA						STEADY STATE					DEPLOYMENT					REMARKS
										DRAG COEFFICIENT							
RUN NO.	PARACHUTE MODEL NO.	CANOPY CLOTH MIL-C-	GAP WIDTH G (in)	BAND BILLOW W_B (in)	BAND LENGTH L_B (in)	DEPLOY TEST	F_{SS} (lb)	q_{SS} (psf)	C_DS_O (ft^2)	DISK AREA C_{DD}	TOTAL AREA C_{DT}	MAX FORCE F_{MAX} (lb)	q @F_{MAX} (psf)	C_DS MAX (ft^2)	SHOCK FACTOR K	AVERAGE SHOCK FACTOR K_{av}	
101	30	7020	4	6 1/16	8	YES	756.5	89.91	8.414	1.496	0.681	813.6	102.49	7.938	0.943	0.956	
102	30	7020	4	6 1/16	8	YES	763.2	90.06	8.474	1.507	0.686	835.1	101.77	8.206	0.968		
103	30	7020	4	6 1/16	4		614.0	100.01	6.139	1.091	0.683						
104	31	7020	6	6 1/16	12		720.6	92.10	7.825	1.391	0.498						
108	31	7020	6	6 1/16	8	YES	699.3	90.71	7.378	1.312	0.597	734.8	102.21	7.189	0.974	1.014	
109	31	7020	6	6 1/16	8	YES	645.1	90.91	7.096	1.261	0.574	763.0	101.97	7.483	1.054		
110	31	7020	6	6 6/16	4		579.3	100.26	5.778	1.027	0.643						
117	32	17208	2	4 9/16	12		481.2	99.91	4.816	0.856	0.364						SLIGHT BAND INFLATION INSTABILITY, see Figure 4
118	32	17208	2	4 9/16	8	YES	468.6	95.94	4.885	1.868	1.457	507.3	101.95	4.976	1.019	1.017	
119	32	17208	2	4 9/16	8	YES	553.9	98.20	5.640	1.003	0.527	587.6	102.65	5.724	1.015		
120	32	17208	2	4 9/16	4		423.2	100.56	4.208	0.748	0.516						
121	32	17208	–	–	0		370.0	100.93	3.666	0.652	0.652						
122	33	17208	4	4 9/16	12		521.2	101.43	5.139	0.914	0.389						
123	33	17208	4	4 9/16	8	YES	528.8	98.36	5.377	0.956	0.503	586.0	102.10	5.739	1.067		
124	33	17208	4	4 9/16	8	YES	517.2	98.33	5.260	0.935	0.492					1.049	
125	33	17208	4	4 9/16	8	YES	524.3	98.31	5.333	0.948	0.499	560.4	101.99	5.494	1.030		
126	33	17208	4	4 9/16	4		530.7	100.75	5.267	0.936	0.646						
127	34	17208	6	4 9/16	12		391.6	102.27	3.829	0.681	0.289						BAND DID NOT FULLY INFLATE
128	34	17208	6	4 9/16	8	YES	480.6	102.45	4.691	0.834	0.439	570.1	102.08	5.585	1.191	1.142	BAND DID NOT FULLY INFLATE
129	34	17208	6	4 9/16	8	YES	464.4	96.61	4.807	0.855	0.450	536.0	102.14	5.247	1.092		BAND DID NOT FULLY INFLATE
130	34	17208	6	4 9/16	4		458.7	100.69	4.556	0.810	0.558						BAND DID NOT FULLY INFLATE, see Figure 4
131	35	17208	2	5 1/16	12		590.0	94.97	6.212	1.104	0.442						
132	35	17208	2	5 1/16	8	YES	613.9	92.67	6.625	1.178	0.589	688.1	102.43	6.718	1.014	1.014	

TABLE 2. SUMMARY OF DISK-GAP-BAND PARACHUTE WIND TUNNEL TEST DATA (Continued)

TABLE 2. SUMMARY OF DISK-GAP-BAND PARACHUTE WIND TUNNEL TEST DATA (Continued)

	MODEL DATA						STEADY STATE					DEPLOYMENT					REMARKS
										DRAG COEFFICIENT							
RUN NO.	PARACHUTE MODEL NO.	CANOPY CLOTH MIL-C-	GAP WIDTH G (in)	BAND BILLOW W_B (in)	BAND LENGTH L_B (in)	DEPLOY TEST	F_{SS} (lb)	q_{SS} (psf)	C_DS_O (ft^2)	DISK AREA C_{DD}	TOTAL AREA C_{DT}	MAX FORCE F_{MAX} (lb)	q @F_{MAX} (psf)	C_DS MAX (ft^2)	SHOCK FACTOR K	AVERAGE SHOCK FACTOR K_{av}	
133	36	17208	4	5 1/16	12		503.4	98.55	5.108	0.908	0.363						
134	36	17208	4	5 1/16	8	YES	574.2	93.71	6.128	1.089	0.545	654.8	102.08	6.415	1.047	1.080	
135	36	17208	4	5 1/16	8	YES	569.5	94.40	6.034	1.073	0.536	685.7	102.12	6.715	1.113		
136	36	17208	4	5 1/16	4		540.8	98.78	5.474	0.973	0.649						
137	37	17208	6	5 1/16	12		554.1	99.30	5.580	0.992	0.397						
138	37	17208	6	5 1/16	8	YES	567.8	95.91	5.921	1.053	0.526	627.2	91.59	6.848	1.157	1.091	BAND DELAYED IN INFLATION, THEN INFLATED FULLY
139	37	17208	6	5 1/16	8	YES	579.2	95.34	6.076	1.080	0.540	635.2	101.99	6.228	1.025		BAND INFLATED NORMALLY
140	37	17208	6	5 1/16	4		529.2	100.63	5.259	0.935	0.623						SLIGHT BAND INFLATION INSTABILITY, see Figure 4
141	38	17208	2	6 1/16	12		731.1	85.79	8.522	1.515	0.542						
142	38	17208	2	6 1/16	8	YES	727.3	85.05	8.551	1.520	0.692	824.7	102.91	8.014	0.937	0.952	
143	38	17208	2	6 1/16	8	YES	721.9	84.84	8.509	1.513	0.688	843.2	102.47	8.228	0.967		
144	38	17208	2	6 1/16	4		540.3	96.07	5.624	1.000	0.625						
145	39	17208	4	6 1/16	12		687.1	90.90	7.559	1.344	0.481						
146	39	17208	4	6 1/16	8	YES	694.3	86.87	7.992	1.421	0.646	809.6	101.99	7.938	0.993	0.991	
147	39	17208	4	6 1/16	8	YES	707.0	86.83	8.143	1.448	0.659	824.1	102.30	8.056	0.989		
148	39	17208	4	6 1/16	4		507.7	97.84	5.190	0.923	0.577						
149	39	17208	–	–	0		430.9	101.66	4.238	0.753	0.753						
150	40	17208	6	6 1/16	12		380.1	101.52	3.744	0.666	0.238						BAND DID NOT INFLATE
151	40	17208	6	6 1/16	8	YES	504.7	101.83	4.956	0.881	0.401	531.4	102.23	5.198	1.049	1.026	BAND DID NOT INFLATE
152	40	17208	6	6 1/16	8	YES	486.2	101.70	4.781	0.850	0.387	492.0	102.43	4.803	1.003		BAND DID NOT INFLATE
153	40	17208	6	6 1/16	4		514.4	102.22	5.033	0.895	0.560						BAND DID NOT INFLATE, see Figure 4
154	40	17208	–	–	0		485.0	103.15	4.702	0.836	0.836						

INFINITE MASS SHOCK FACTOR

$$F_1 = F_{SS} \left(\frac{q_{@F_{max}}}{q_{SS}} \right)$$

The infinite mass shock factor is defined as the ratio of the maximum deployment force to the steady-state drag force at the same dynamic pressure. The steady-state drag must be adjusted for the variation between the dynamic pressure at F_{max} and the steady-state condition.

Adjusted drag force

Infinite mass shock factor

$$K = \frac{F_{max}}{F_1}$$

Shock factors are presented in Table 2.

CANOPY DESIGN DIAMETER, D_O

The constant disk surface area, SD = 810 in^2

$$D_o = \sqrt{\frac{4S_D}{\pi}}$$

$$D_o = \sqrt{\frac{4 \times 810}{\pi}}$$

$$D_o = 32.1142 \text{ inches}$$

A summary of normalized gap lengths, G/D_O, band lengths, L_B/D_O, and band widths, W_B/D_O, is presented in Figure 1.

TEST RESULTS

The most efficient parachute design provides acceptable stability and opening force limits, together with a maximum drag area obtained from a minimum of canopy cloth. The cloth permeability, gap length, band length, and band billow width produce numerous mutually related effects on the Disk-Gap-Band parachute drag area, stability, inflation characteristics, and opening force performance. The reader should keep in mind that in order to structure a narrative explanation of the test results, the four mutually related performance areas are discussed separately, but act concurrently.

DISCUSSION OF THE VARIATION OF DRAG AREA WITH THE SEVERAL TEST PARAMETERS

Figure 2 presents the interrelated effects of cloth permeability, P; gap length, G; band length L_B; and gore billow width, W_B; on the parachute steady state drag area, C_DS_O. An examination of Figure 2 provides the following general conclusions:

a. Reading Figure 2 horizontally for a constant cloth permeability shows that the steady state drag area generally decreases as the gap is widened from 2 inches to 6 inches.

b. Reading Figure 2 vertically for a constant gap width and a varying cloth permeability shows that as the cloth permeability increases the parachute steady-state drag area generally decreases.

c. As the band billow, W_B, increases the steady-state drag area increases. Additional band billow may be desirable to further improve the drag area. The 4-9/16-inch-band billow was selected as smaller than the disk gore hem dimension of 5-1/16 inches. The test data indicate that the reduction of the band billow substantially restricts the parachute drag producing effectiveness. The discussion of the test data is to be limited to the optimum test band billow value of $W_B = 6\ 1/16$ inches.

d. The maximum steady-state drag area generally occurs for a band length of 8 inches, ($L_B/D_O = 0.2491$). The notable exception is the MIL-C-7020 cloth with the 2-inch and 6-inch gaps. The 4-inch gap data shows essentially equal steady-state drag areas for band lengths of 8 inches ($L_B/D_O = 0.2491$) and 12 inches ($L_B/D_O = 0.3737$). However, the change in steady-state drag area does not warrant the additional cloth required. The same comments are applicable to the 4-inch gap data. Here is an example of improving the design efficiency with a minimum of cloth utilization:

The drag area of the MIL-C-7020 cloth parachute with a 12-inch-band length exceeds the drag area of the 8-inch-band length by 8.2 percent. This increase in drag area may be achieved two ways.

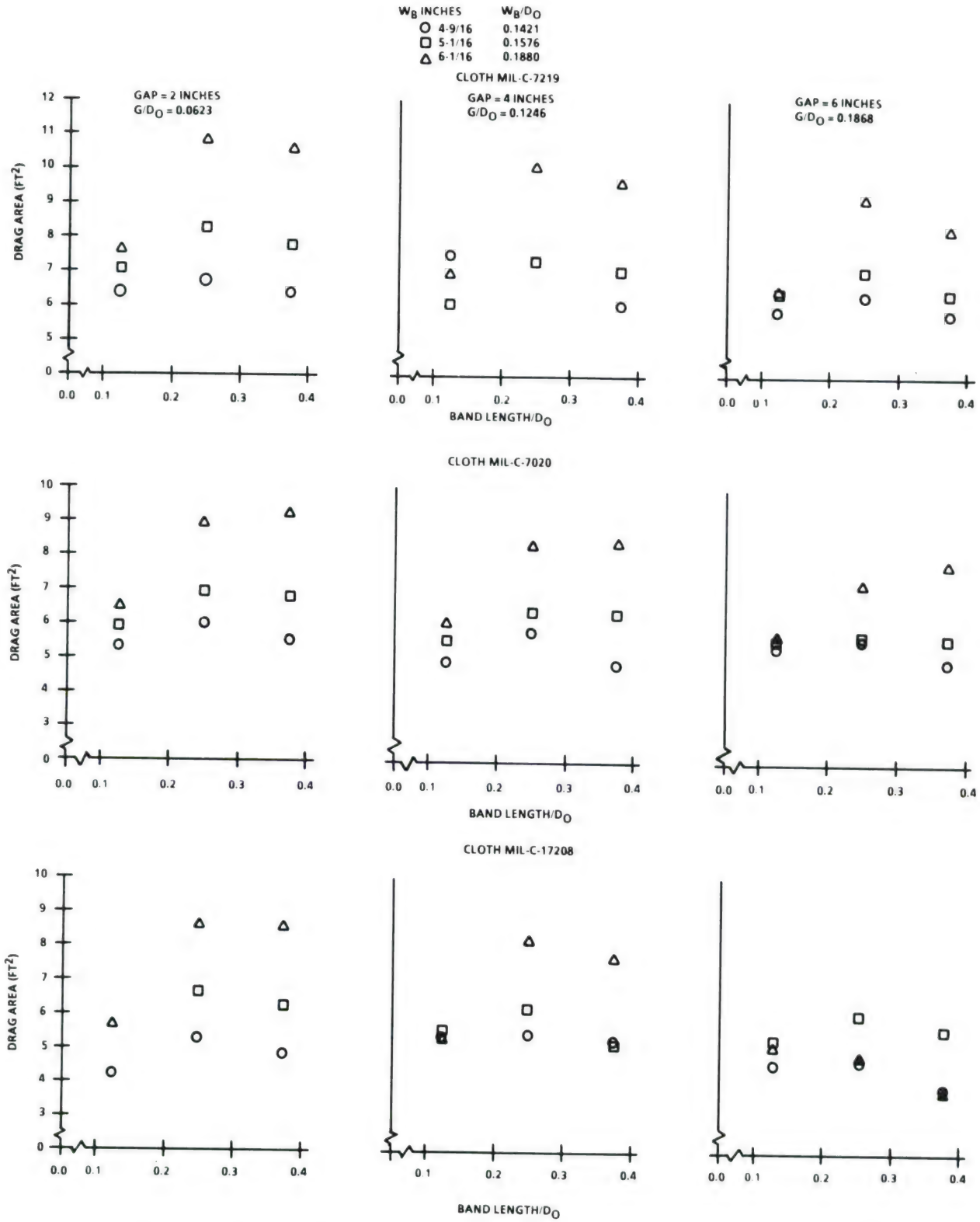

FIGURE 2. EFFECTS OF GAP LENGTH AND BAND LENGTH ON THE PARACHUTE DRAG AREA FOR VARIOUS BAND BILLOW ALLOWANCES

a. Use the 12-inch-band length. In this case the total cloth areas, ST, from Figure 1 are 15.729 ft^2 for the 12-inch-band length and 12.361 ft^2 for the 8-inch-band length.

$$\text{Total area ratio} = \frac{15.729}{12.361} = 1.27$$

With this approach, the 8.2-percent drag area increase requires a 27-percent increase in the parachute total cloth area.

b. A better design method is to increase the D_O diameter of the parachute by 4 percent and design a slightly larger parachute.

$$\text{Drag area increase factor} = \sqrt{1.082} = 1.040$$

then:

New diameter

$$D_o = 1.04 \times 32.1142$$

$$D_o = 33.3988 \text{ inches}$$

New billow width

$$W_B = \frac{W_B}{D_o} \times D_o$$

$$W_B = 0.1888 \times 33.3988$$

$$W_B = 6.305 \text{ in.}$$

New band length

$$L_B = \frac{L_B}{D_O} \times D_o$$

$$L_B = 0.2491 \times 33.3988$$

$$L_B = 8.32 \text{ in.}$$

New Band Area

$$S_B = \frac{NW_B L_B}{144}$$

$$S_B = \frac{20W_B L_B}{144}$$

$$S_B = 7.286 \text{ ft}^2$$

New Disk Area

$$S_D = \frac{\pi D_o^2}{4 \times 144}$$

$$S_D = \frac{\pi 33.3988^2}{4 \times 144}$$

$$S_D = 6.084 \text{ ft}^2$$

New Total Cloth Area

$$S_T = S_B + S_D$$

$$S_T = 6.084 + 7.286$$

$$S_T = 13.370 \text{ ft}^2$$

Total Cloth Area Increase

$$\text{Total area ratio} = \frac{13.370}{12.361} = 1.082$$

Adding area to the efficient drag-producing disk rather than only to the inefficient drag-producing stabilization band is the best approach to minimum cloth design of Disk-Gap-Band parachutes. Figure 3 is a replot of the drag area data as a function of cloth permeability. The increase in drag area as the band billow, W_B,

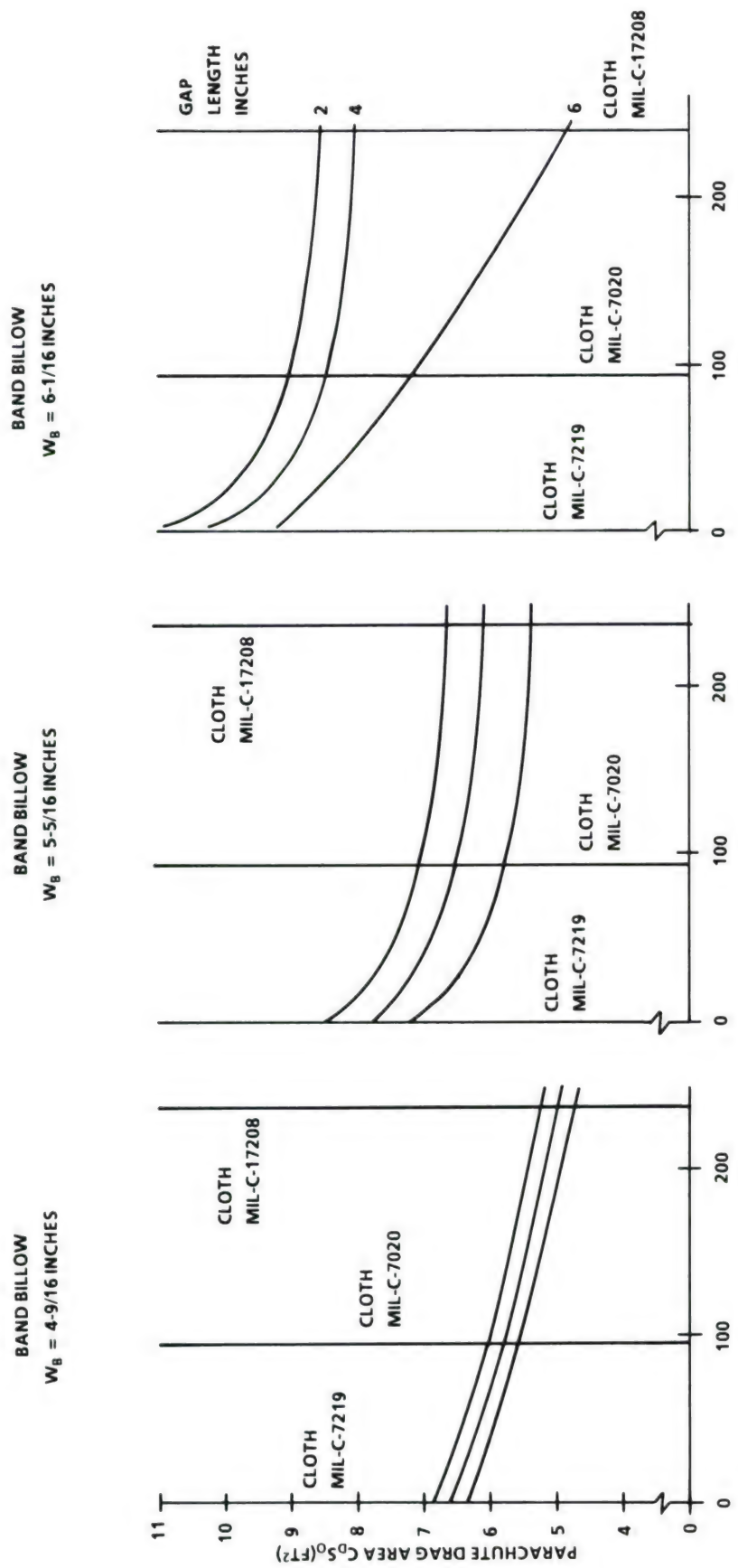

FIGURE 3. EFFECTS OF CLOTH PERMEABILITY, GAP LENGTH, AND BAND BILLOW ON THE DISK-GAP-BAND PARACHUTE DRAG AREA FOR L_B = 8 INCHES, L_B/D_O = 0.2491

increases and the reduction of drag area with increasing gap length, G, and cloth permeability, P, are evident. The drag areas have a uniformity of variation except for the 6-1/16-inch-band billow width with a 6-inch-gap length. The 2- and 4-inch-gap lengths show a variation similar to the 4-9/16- and 5-1/16-inch-band widths. Extending the gap to 6 inches, for $W_B = 6\text{-}1/16$ inches, results in a reduction of drag area for the MIL-C-7020 cloth and the MIL-C-17208 cloth. The 6-inch gap MIL-C-7020 cloth configuration experienced failure of the band to inflate in run number 105 while all of the 6-inch gap MIL-C-17208 band configurations (runs 150 thru 154) failed to inflate. Figure 4 is a composite of photographs of the 27 test models in the steady-state drag condition. Note how the parachute alignment relative to the wind tunnel center line and band inflation characteristics change as the cloth permeability and gap length increases.

The definition of parachute stability is a parachute that tends to return to the system center line when it is deflected. The MIL-C-7219 cloth parachutes of Figure 4 are considered as unstable under this definition. The remaining parachutes are stable and oscillate at small angles to the center line. The theoretical approach to Disk-Gap-Band parachutes is included in Reference 1.

Low permeability cloths generate internal pressure sufficiently high to fully inflate the canopy band for all gap lengths and band billow widths. The lack of airflow through the canopy cloth results in the development of destabilizing lift forces which deflect the parachute from the wind tunnel centerline. Figure 5 compares one cycle of motion of a flat circular parachute and a Disk-Gap-Band parachute. Both models are constructed using MIL-C-7219 cloth in order to maximize the instability effects. The Disk-Gap-Band parachute design possesses improved inherent lift control which reduces the canopy tendency to deviate from the trajectory. The sustained motion of the flat circular canopy was mainly a coning motion at the maximum pitch angle while the Disk-Gap-Band parachute mainly oscillated. Additional airflow through the canopy controls the destabilizing lift force and reduces the maximum angle of oscillation of the parachute.

Figure 6 presents the maximum oscillation angles measured from motion picture coverage for the several models with $L_B = 8$ inches. Extending the gap length generally reduces the maximum angle of oscillation for all values of W_B. The minimum oscillation angles are experienced by the MIL-C-17208 cloth parachutes. As the canopy rate of airflow is augmented, the internal pressure is reduced. The MIL-C-17208 cloth can propagate internal pressure to inflate the band with gap lengths of 2 inches and 4 inches. Extension of the gap to 6 inches results in an uninflated band because the pressurized zone cannot propagate past the gap. Increasing the gore billow, W_B, provides additional area for outflow from the band which also contributes to lack of inflation. Most of the Disk-Gap-Band parachute oscillations were less than the maximum angles.

CANOPY CLOTH MIL-C-7219, TYPE I
PERMEABILITY = 5.2 CFM/FT^2

GAP WIDTH (IN)	BAND BILLOW (IN)		
	4 9/16	5 1/16	6 1/16
2	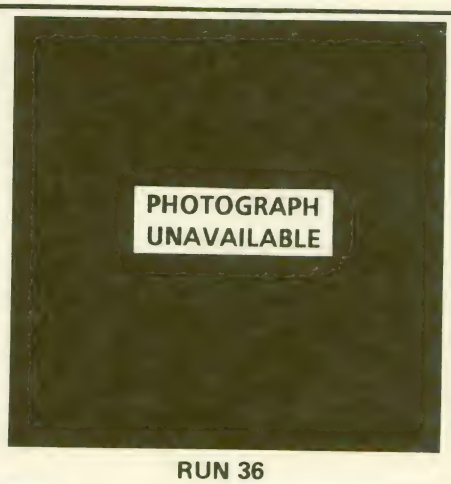 RUN 36	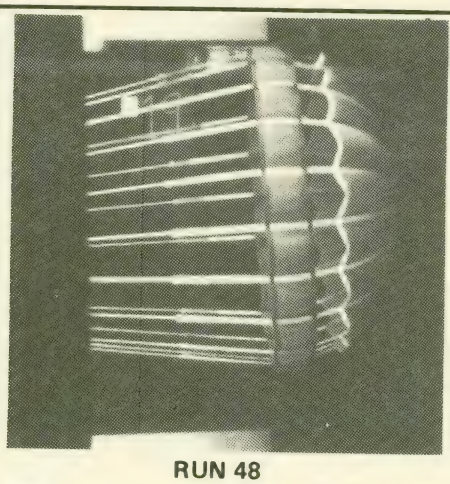 RUN 48	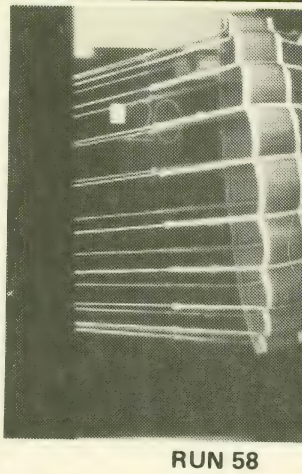 RUN 58
4	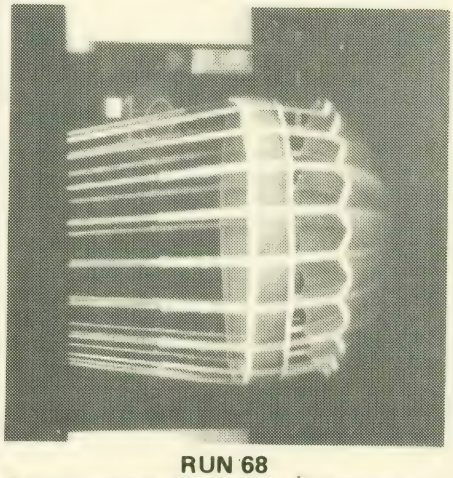 RUN 68	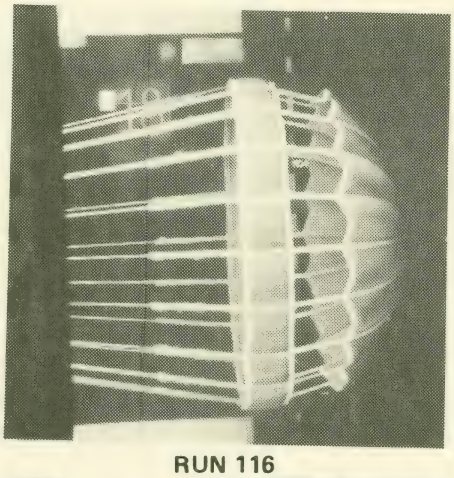 RUN 116	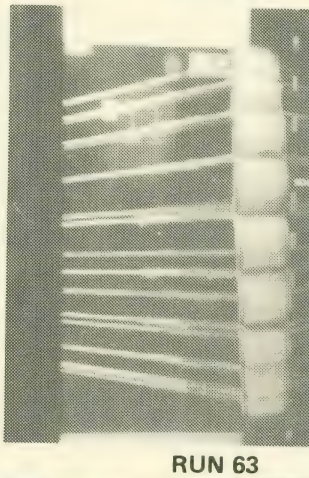 RUN 63
6	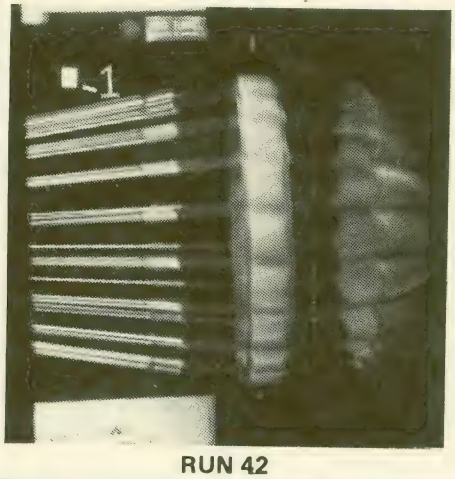 RUN 42	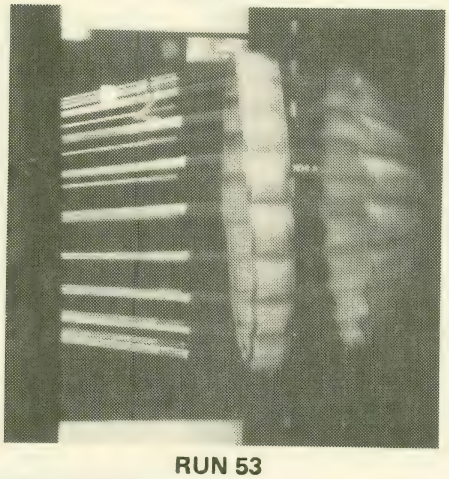 RUN 53	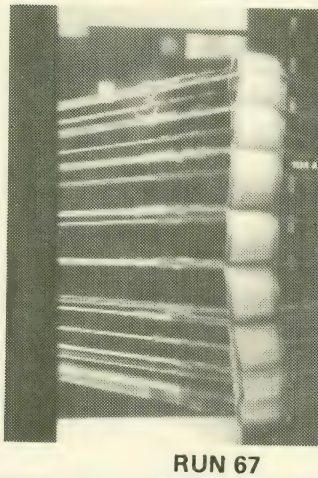 RUN 67

CANOPY CLOTH MIL-C 7020, TYPE I
PERMEABILITY = 93.9 CFM/FT^2

GAP WIDTH (IN)	BAND BILLOW (IN) 4 9/16	5 1/16	6 1/16
2	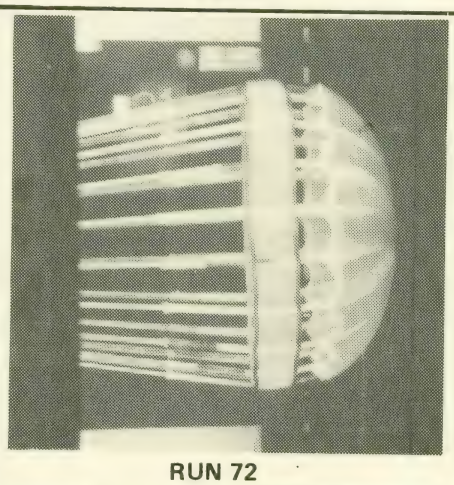 RUN 72	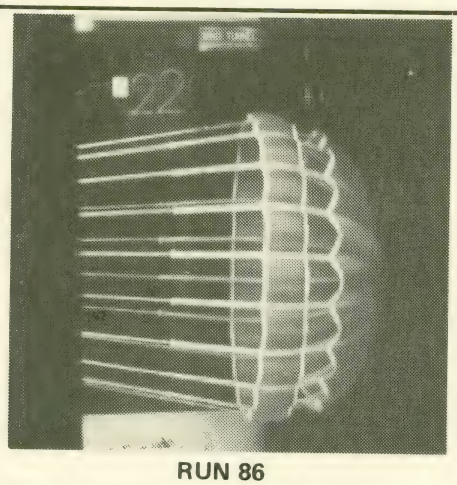 RUN 86	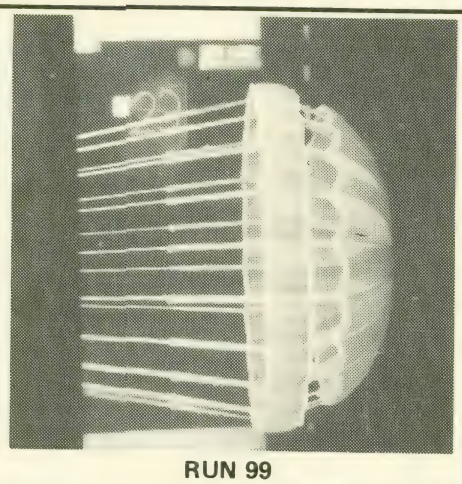 RUN 99
4	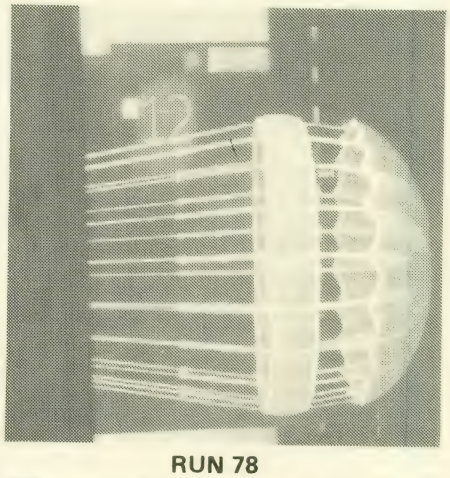 RUN 78	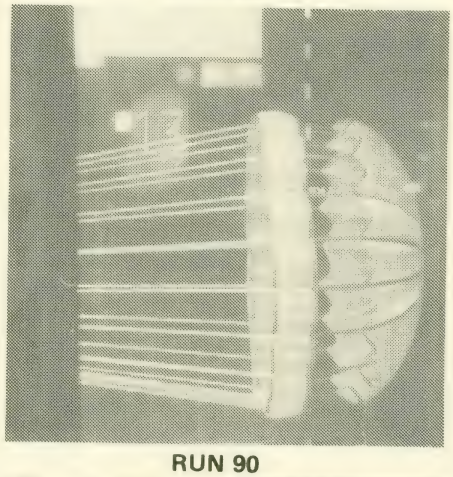 RUN 90	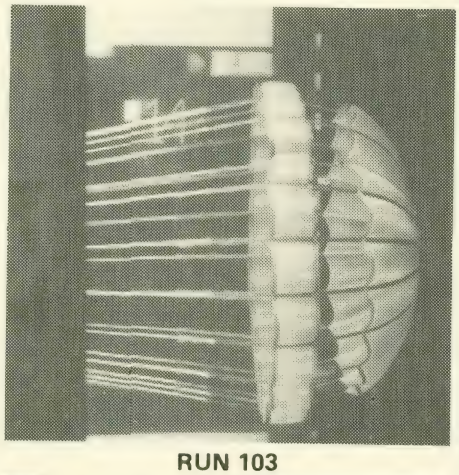 RUN 103
6	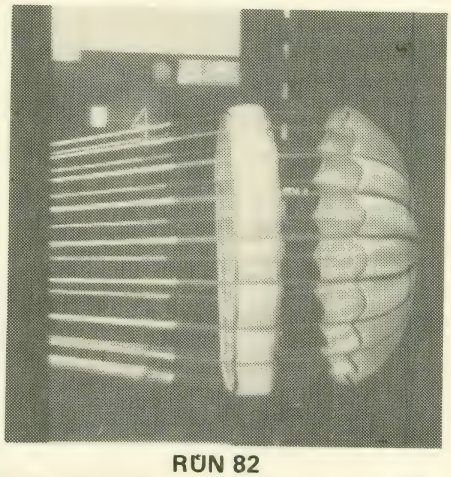 RUN 82	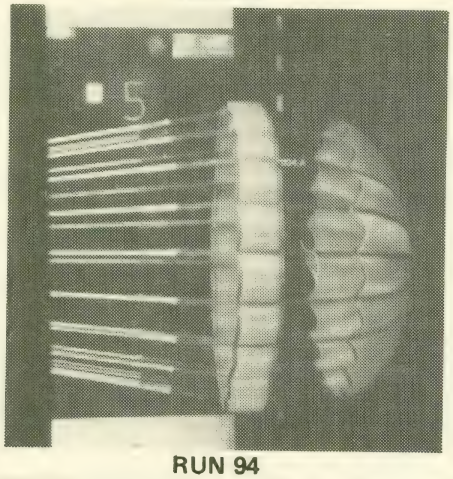 RUN 94	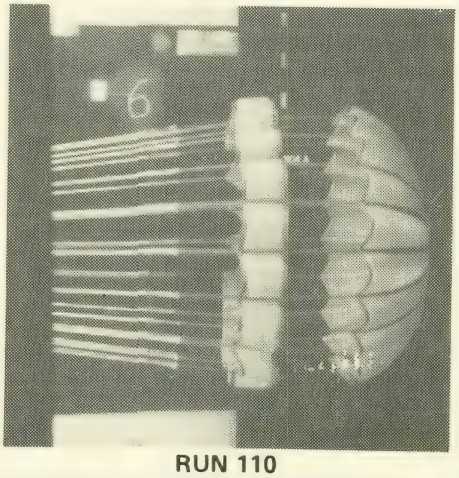 RUN 110

CANOPY CLOTH MIL-C-17208, TYPE I, CLASS C
PERMEABILITY = 237.0 CFM/FT^2

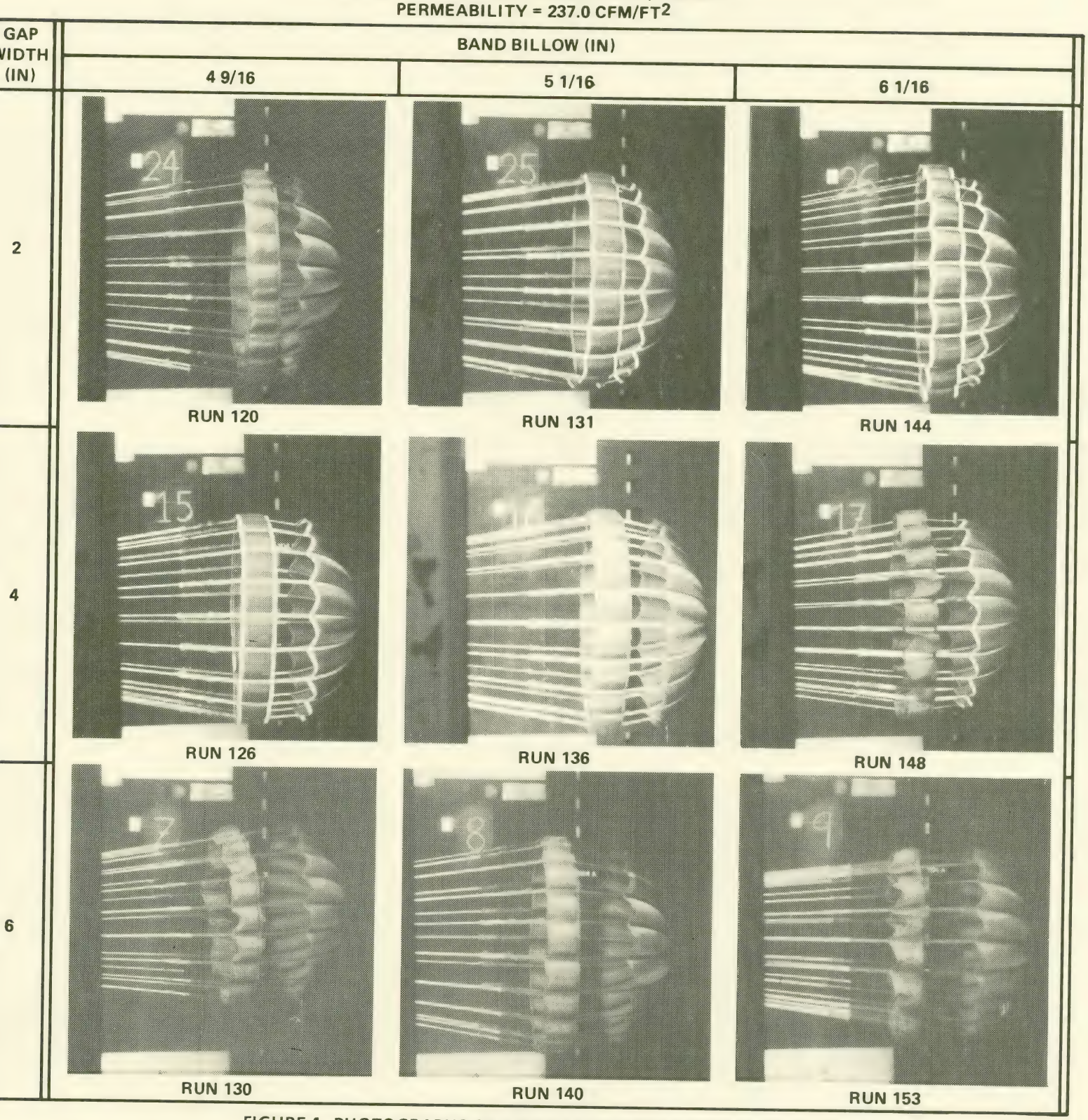

FIGURE 4. PHOTOGRAPHS OF STEADY STATE INFLATED PARACHUTE CANOPIES WITH A BAND LENGTH OF 4 INCHES. NOTE THE EFFECTS OF CLOTH PERMEABILITY ON THE ALIGNMENT OF THE PARACHUTES WITH THE WIND TUNNEL CENTER LINE AND THE FULLY INFLATED CANOPY SHAPE

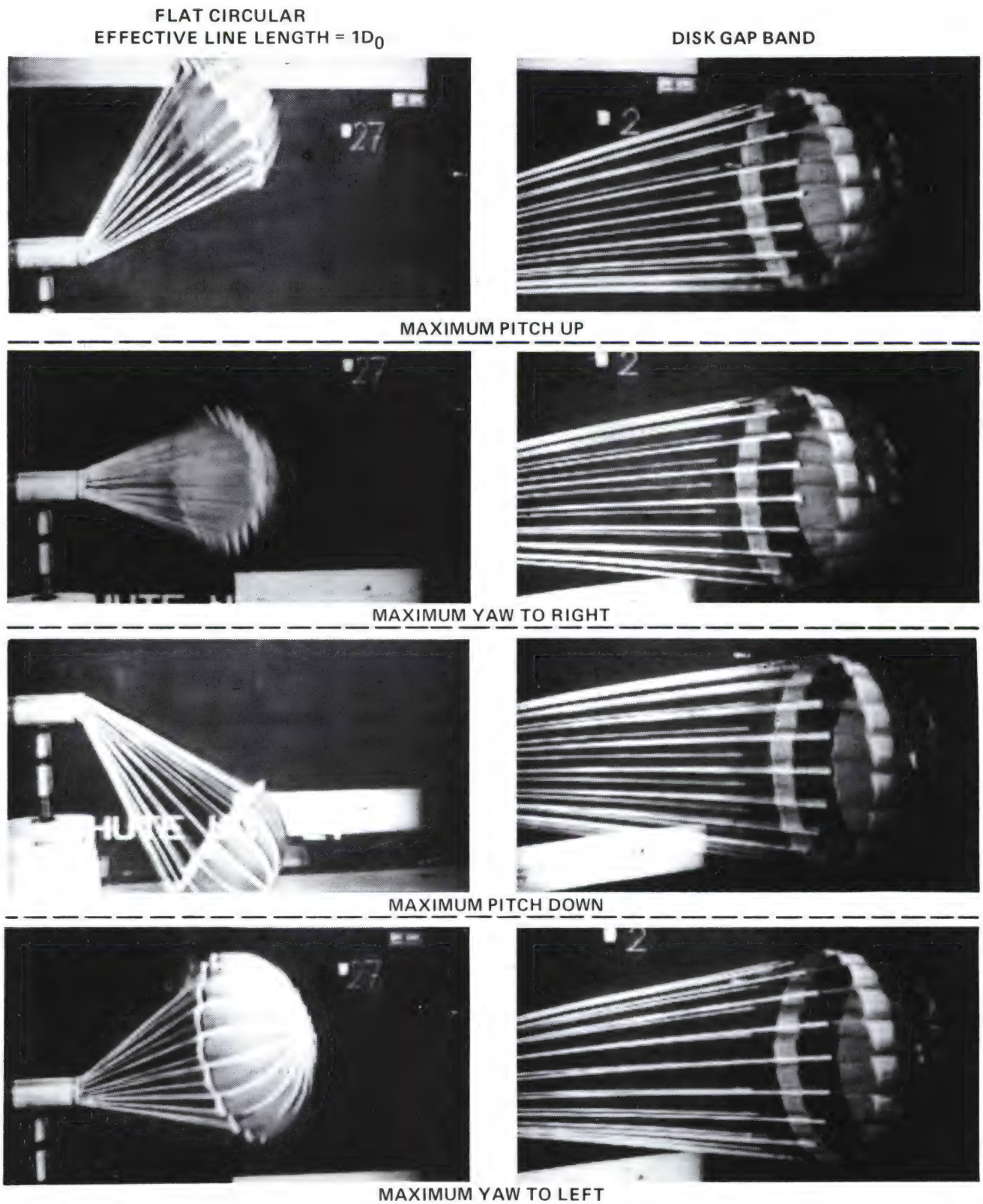

FIGURE 5. COMPARISON OF THE OSCILLATIONS OF THE SOLID CLOTH FLAT CIRCULAR AND DISK GAP BAND PARACHUTES AT 150 MPH

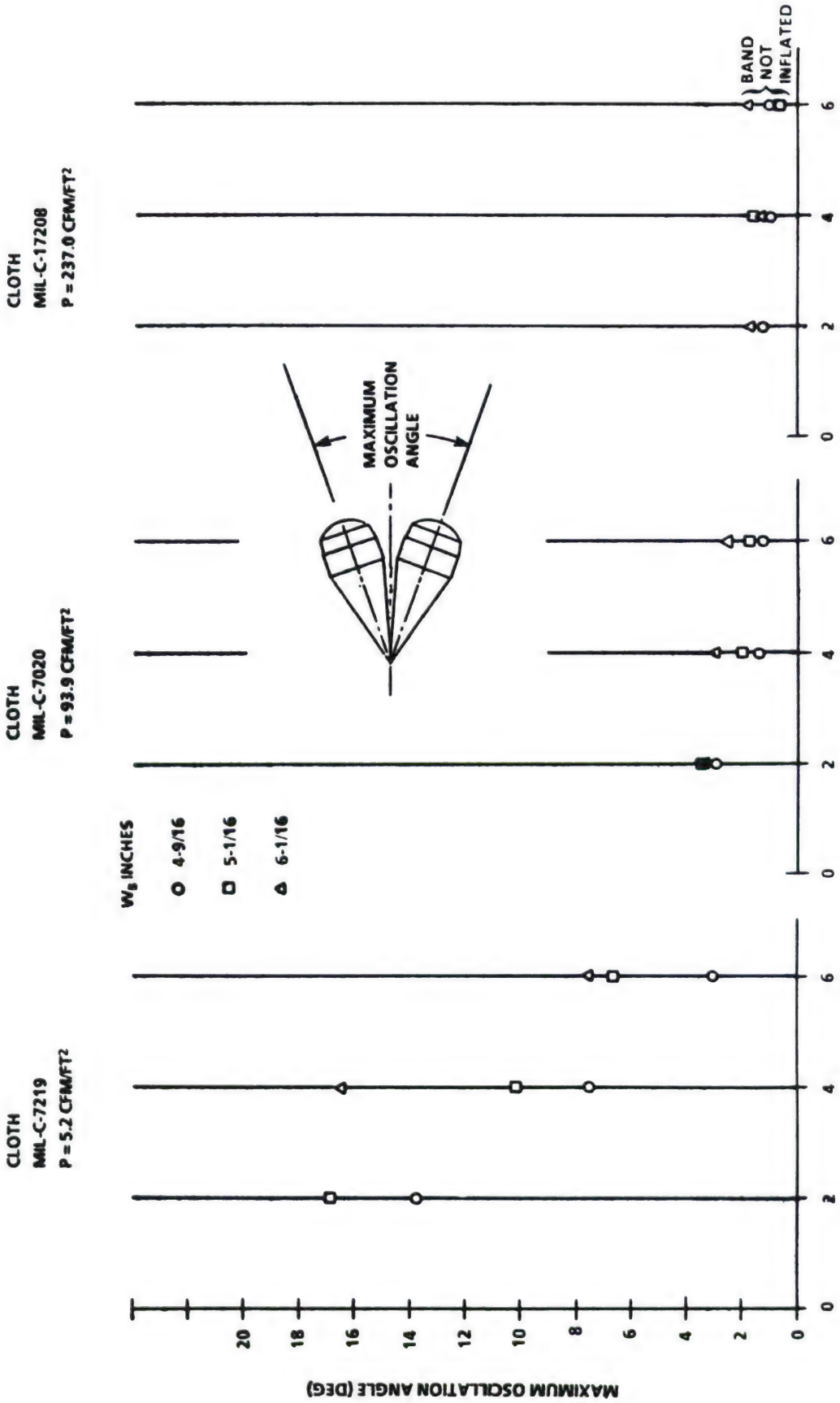

FIGURE 6. EFFECTS OF CLOTH PERMEABILITY, GAP LENGTH, AND BAND BILLOW ON THE MAXIMUM OSCILLATION ANGLE OF THE SEVERAL PARACHUTES FOR AN L_B = 8 INCHES

OPENING SHOCK FACTOR

For each of the infinite mass opening shock tests, the parachute was packed within the test stand. When the wind tunnel velocity reached a steady-state of 200 mph, a small inflated extraction parachute was released to deploy the test parachute. The force sensors in the test stand were electrically connected to the wind tunnel recording instrumentation which made continuous records of parachute force and wind tunnel dynamic pressure as a function of time. Figure 7 shows several typical examples of the data presentation which were selected at random. The upper trace records the instantaneous wind tunnel dynamic pressure and the lower trace is the opening force variation. Each parachute deployment took place at constant wind tunnel velocity. After inflation the parachute caused some reduction in the wind tunnel velocity. The velocity was returned to approximately 200 mph and the mean steady-state values determined. The infinite mass shock factors for each test were calculated by the data reduction formulas and are listed in Table 2.

The DGB parachute exhibits a dynamic drag area signature that is linear during the inflation process. Figure 8 is an expanded printout to illustrate the linearity of the dynamic drag area during inflation. This is a considerably different inflation characteristic compared to the flat circular parachute. The opening shock factors are much less than the 1.8 to 2.0 usually expected with solid cloth parachutes. Of the fifty-three deployment tests conducted, individual opening shock factors exceeded 1.15 in seven of the tests (runs 40, 41, 61, 84, 93, 128, 138). The limited test data for each configuration was averaged together and tabulated in Table 3 together with the one sigma variation. After the averaging process only 3 values exceed 1.15. Test runs 35, 151, and 152 had oscillations of the steady-state drag force that exceeded the maximum opening force. The average shock factors of Table 3 are plotted in Figure 9. The reduction of the shock factor as the cloth permeability increases is evident.

CANOPY CLOTH MIL–C–7219, TYPE I

RUN NO. 34, MODEL NO. 14
G = 2 IN.; $W_B = 4\frac{9}{16}$ IN.; $L_B = 8$ IN.; $C_DS_O = 6.76$ FT^2

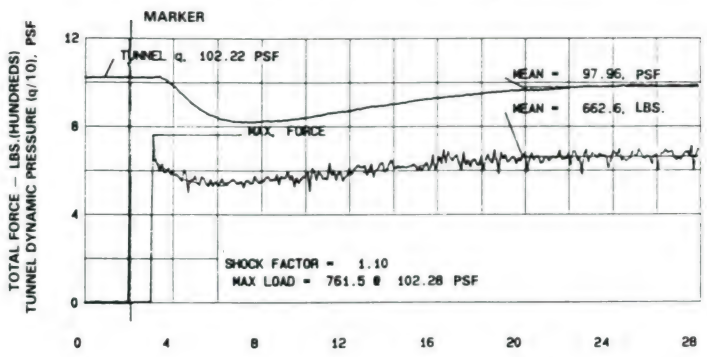

RUN NO. 113, MODEL NO. 18
G = 4 IN.; $W_B = 5\frac{1}{16}$ IN.; $L_B = 8$ IN.; $C_DS_O = 7.57$ FT^2

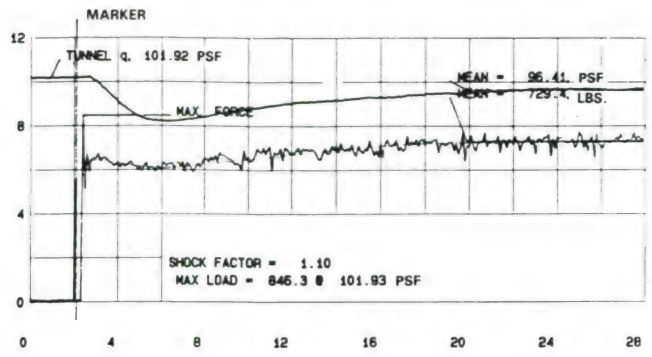

RUN NO. 65, MODEL NO. 22
G = 6 IN.; $W_B = 6\frac{1}{16}$ IN.; $L_B = 8$ IN.; $C_DS_O = 8.75$ FT^2

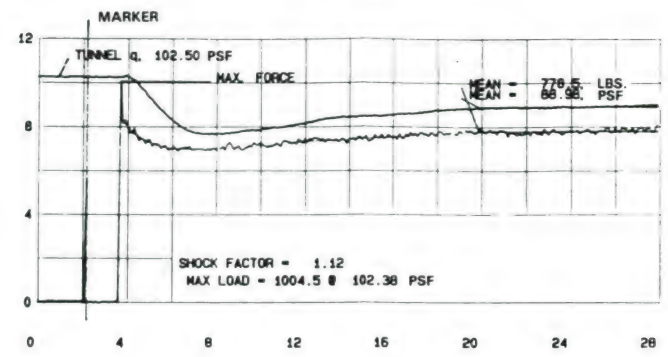

CANOPY CLOTH MIL–C–7020, TYPE I

RUN NO. 84, MODEL NO. 26
G = 2 IN.; $W_B = 5\frac{1}{16}$ IN.; $L_B = 8$ IN.; $C_DS_O = 7.38$ FT^2

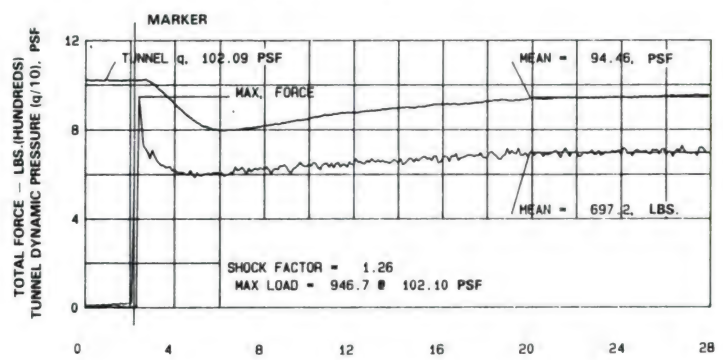

RUN NO. 102, MODEL NO. 30
G = 4 IN.; $W_B = 6\frac{1}{16}$ IN.; $L_B = 8$ IN.; $C_DS_O = 8.47$ FT^2

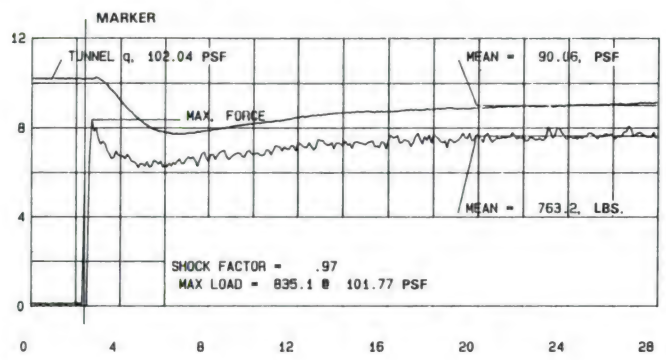

RUN NO. 80, MODEL NO. 25
G = 6 IN.; $W_B = 4\frac{9}{16}$ IN.; $L_B = 8$ IN.; $C_DS_O = 5.77$ FT^2

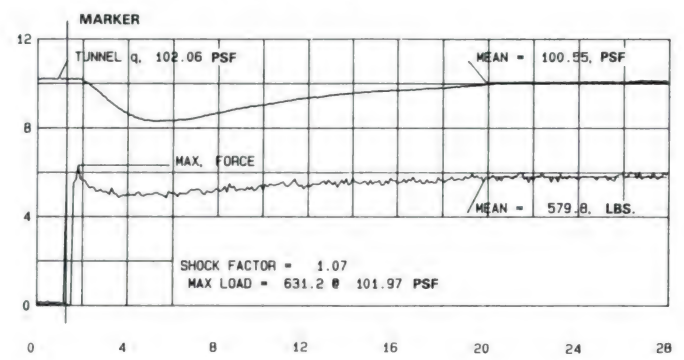

CANOPY CLOTH MIL–C–17208, TYPE I, CLASS C

RUN NO. 143, MODEL NO. 38
G = 2 IN.; $W_B = 6\frac{1}{16}$ IN.; $L_B = 8$ IN.; $C_DS_O = 8.51$ FT^2

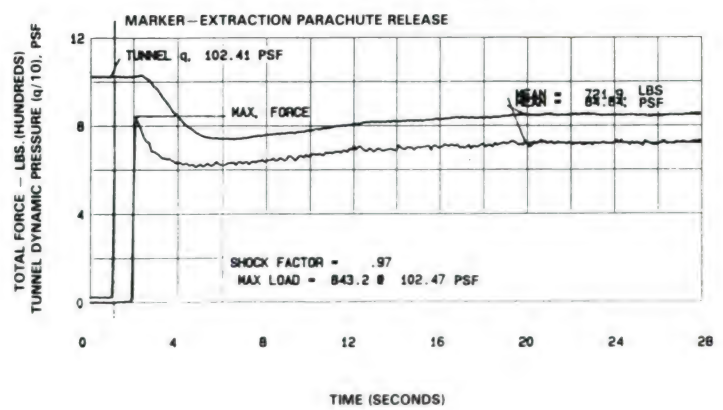

RUN NO. 125, MODEL NO. 33
G = 4 IN.; $W_B = 4\frac{9}{16}$ IN.; $L_B = 8$ IN.; $C_DS_O = 5.33$ FT^2

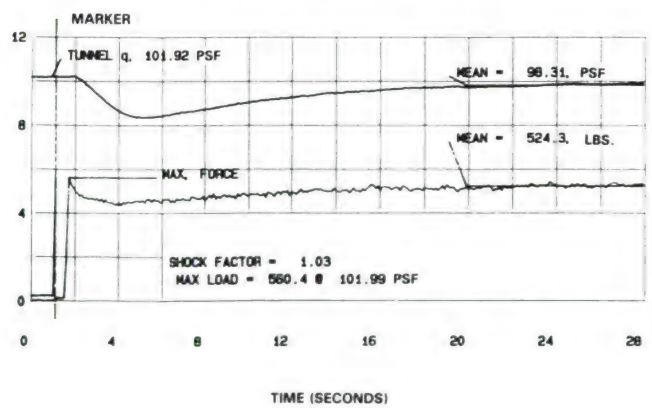

RUN NO. 138, MODEL NO. 37
G = 6 IN.; $W_B = 5\frac{1}{16}$ IN.; $L_B = 8$ IN.; $C_DS_O = 5.92$ FT^2

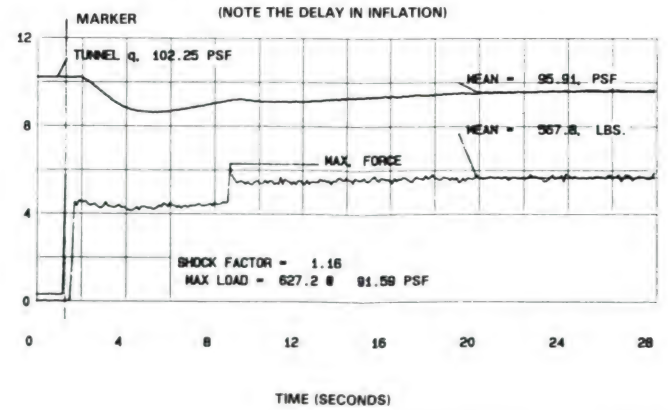

FIGURE 7. TYPICAL PARACHUTE OPENING FORCE TEST RECORDS

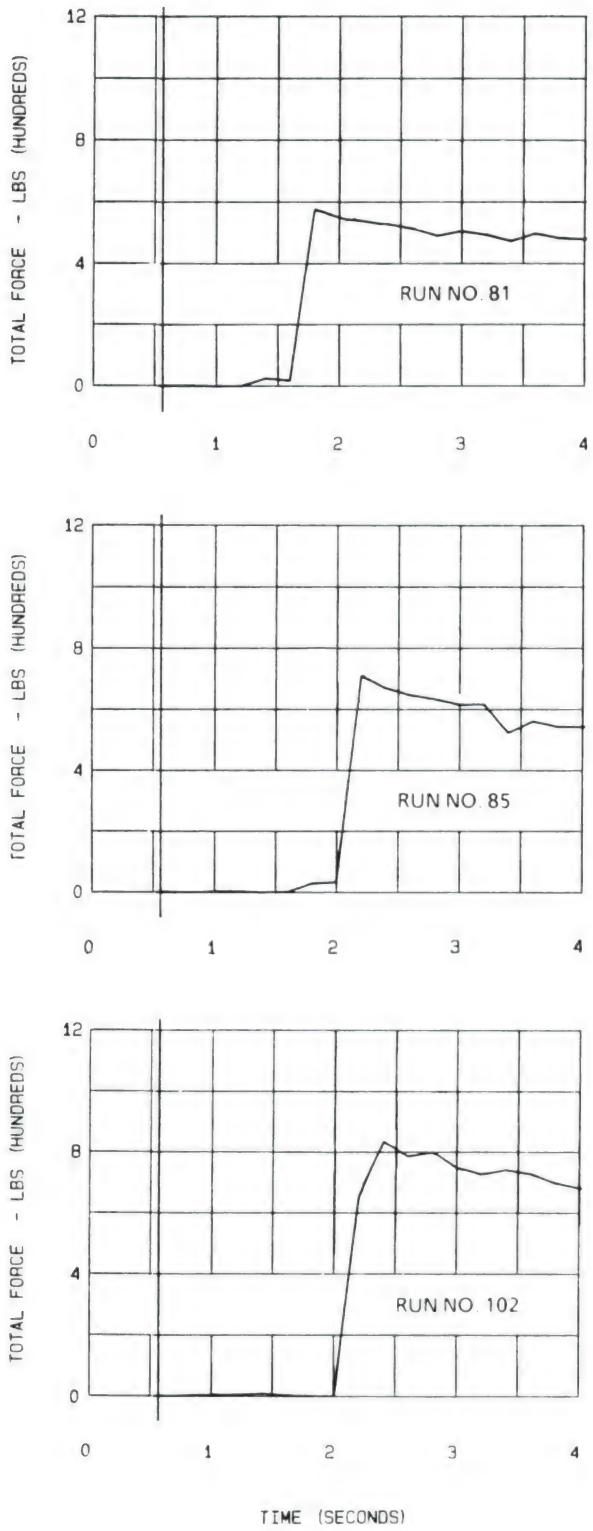

FIGURE 8. EXPANDED OPENING SHOCK SIGNATURES TO DEMOSTRATE LINEARITY OF DRAG AREA DURING INFLATION

TABLE 3. SUMMARY OF AVERAGE OPENING SHOCK FACTORS FOR ALL CONFIGURATIONS L_B = 8 INCHES, L_B/D_O = 0.2491

BAND BILLOW W_B (IN) / GAP LENGTH G (IN)	4 9/16	5 1/16	6 1/16	AVERAGE K AT CONSTANT GAP LENGTH ± 1σ	AVERAGE K FOR CONSTANT CLOTH ± 1σ	AVERAGE K OF ALL TESTS ± 1σ
	CLOTH MIL-C-7219, TYPE I PERMEABILITY = 5.2 CFM/FT²					
2	1.07	1.09	1.04	1.07 ±0.02		
4	1.13	1.08	1.16	1.12 ±0.04	1.13 ±0.11	
6	1.41	1.10	1.11	1.21 ±0.18		
AVERAGE K@ CONSTANT BAND BILLOW 1σ	1.24 ±0.18	1.09 ±0.01	1.10 ±0.06			
	CLOTH MIL-C-7020, TYPE I PERMEABILITY = 93.9 CFM/FT²					
2	1.05	1.15	1.00	1.07 ±0.08		
4	1.08	1.02	0.96	1.01 ±0.06	1.05 ±0.06	1.07 ±0.09
6	1.05	1.13	1.01	1.07 ±0.06		
AVERAGE K@ CONSTANT BAND BILLOW 1σ	1.06 ±0.01	1.10 ±0.07	0.99 ±0.03			
	CLOTH MIL-C-17208, TYPE I, CLASS C PERMEABILITY = 237.0 CFM/FT²					
2	1.02	1.01	0.95	0.99 ±0.04		
4	1.05	1.08	0.99	1.03 ±0.04	1.04 ±0.06	
6	1.14	1.09	1.03	1.09 ±0.06		
AVERAGE K@ CONSTANT BAND BILLOW 1σ	1.06 ±0.07	1.06 ±0.04	0.99 ±0.04			

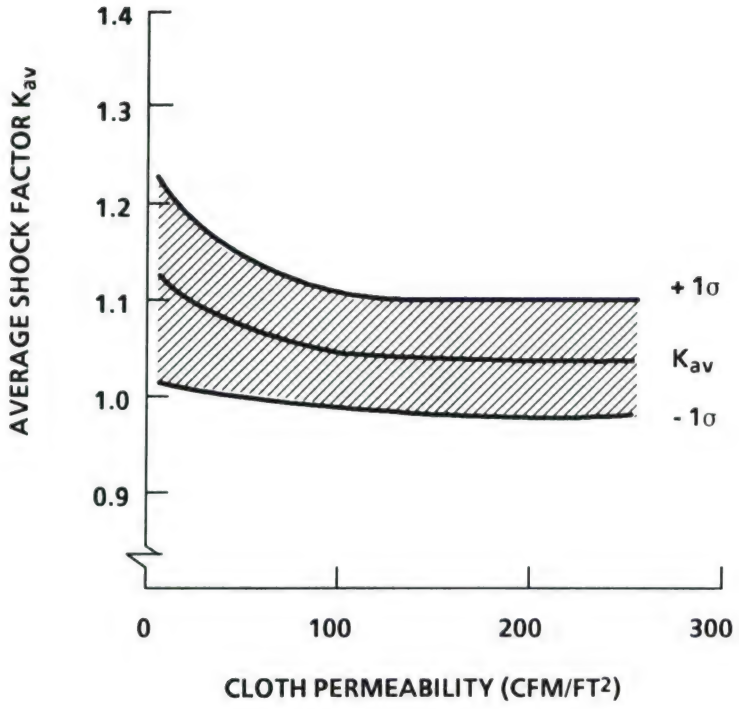

FIGURE 9. AVERAGE SHOCK FACTOR VERSUS CLOTH PERMEABILITY WITH 1 SIGMA VARIATION

DISCUSSION

The results of these tests indicate that the drag area, maximum oscillation angle, inflation characteristics and opening shock forces are dependent upon the cloth permeability, length of the gap, and the amount of billow allowance in the band. Due to financial and wind tunnel testing time restraints, the effort was limited to evaluating canopies of twenty gores. The steady-state aerodynamic drag force and oscillation stability were measured for all of the configurations. However, the opening shock forces were obtained only for canopies with a band length of eight inches.

The linearity of the dynamic drag area during the inflation process and the relatively low infinite mass opening shock factors demonstrate that the Disk-Gap-Band parachute performs in a significantly different manner than the solid cloth parachute from which it was derived. In most designs the aim is to maximize the drag area of the canopy using a minimum of cloth for a configuration that is capable of sustaining the applied design opening shock forces and achieve adequate system stability. Canopy cloths or films with low permeability can be used to maximize parachute drag area. The oscillation of low permeability canopies can be controlled by increasing the length of the gap. Figure 6 illustrates the maximum oscillation angle measured from test motion picture coverage. Note that the maximum angle was measured to the outermost suspension lines for convenience of reference. The oscillation angle of the parachute center line is less than the maximum angles. Most of the oscillation angles were less than the recorded maximum angles. Another approach to increasing the drag area is to add billow to the band width, although this does give some small increase in the maximum oscillation angle. The maximum oscillation angle generally decreases as the canopy permeability increases.

Figures 2 and 3 show the effects of cloth permeability, gap length, and band billow on the parachute drag area. As the band billow increases, the drag area increases. Inflation instability is apparent in the MIL-C-7020 and MIL-C-17208 cloths for a gap length of six inches. In Figure 4, photographs of inflated parachute shapes of the several configurations show the inflation characteristics of the steady-state condition. Note the less obvious band inflation instability in runs 110 and 148. The band length of all Figure 4 parachutes is four inches.

Figure 5 compares one cycle of oscillation stability of a low permeability 20-gore solid cloth parachute, with a one D_0 suspension line length, to a DGB parachute. The DGB parachute was generated by adding a 4-inch-long band spaced at a length of six inches from the solid cloth canopy hem. This modification produces a dramatic change in the oscillation characteristics of the parachute. The suspension line length for the DGB parachute includes the canopy central disk diameter, plus two band lengths, plus two gap lengths. The various dimensions of the model parachutes used in this test; i.e., band length and billow gap length, etc., have been normalized to the model parachute disk D_0 for scaling purposes and are listed in Figure 1.

Instantaneous opening shock force-time data and wind tunnel dynamic pressure during inflation were recorded by the wind tunnel instrumentation. Figure 7 is a graphical print out of randomly selected deployments. The wind tunnel dynamic pressure remained constant during the inflation process indicating true infinite mass deployment. After inflation, the parachute caused the wind tunnel velocity and the dynamic pressure to vary. The operator raised the velocity to a steady-state value. Figure 8 is an expanded time axis of the inflation process and shows the linear variation of the dynamic drag area. Infinite mass opening shock factors are presented in Figure 9. The test data and results are tabulated in Table 2.

CONCLUSIONS

1. The Disk-Gap-Band parachute performs in a significantly different manner than the solid cloth parachute from which it was derived.

2. The parachute drag area, maximum oscillation angle, inflation characteristics and opening shock forces depend upon the cloth permeability, length of the gap, length of the band, and the amount of billow allowance in the band.

3. The dynamic drag area signature during inflation is linear.

4. The drag area can be raised by decreasing the cloth permeability, increasing the band billow, and decreasing the gap length.

5. The oscillation stability of the DGB parachute is significantly improved over a conventional solid flat circular parachute with the same canopy cloth permeability.

6. Adding width to the band billow causes a minor increase in the maximum oscillation angle.

7. The maximum oscillation angle may be decreased by increasing the cloth permeability and/or increasing the gap length. The band length may also affect performance, but was not demonstrated in these tests.

8. Inflation stability depends upon cloth permeability, gap length, and band billow.

9. The DGB parachute infinite mass opening shock factors are relatively low and decrease as the canopy permeability increases.

10. The recommended suspension line length for DGB parachutes is the diametrical distance from the skirt hem of the band to the opposite skirt hem of the band and includes 2 band lengths, plus 2 gap lengths, plus the diameter of the central disk.

11. The investigation was limited to parachutes of twenty gores. Opening shock measurements were obtained from only canopy configurations of 8-inch-band length. Further tests of these variables should be conducted.

NOMENCLATURE

C_{DD}	Drag coefficient referenced to area of disk
C_{DT}	Drag coefficient referenced to total canopy cloth area
C_DS_O	Parachute steady state aerodynamic size, FT^2
D_O	Diameter of a circle having the same area of the disk as the 20 triangular disk gore sections, FT
F	Adjusted steady state drag force at the snatch force dynamic pressure, LB.
F_1	Adjusted steady state drag force at the maximum force dynamic pressure, LB.
F_{max}	Peak force at deployment, LB.
F_{SS}	Steady state drag force, LB.
G	Length of the parachute gap, IN.
K	Infinite mass deployment shock factor
L_B	Length of band, IN.
N	Number of gores in the canopy
P	Cloth rate of airflow under a pressure differential of 1/2 inch of water, CFM/FT^2
q	Dynamic pressure, ρV^2, LB/FT^2
q_{ss}	Steady-state dynamic pressure, LB/FT^2
R	Canopy disk constructed radius, IN.
S_B	Canopy band area, FT^2
S_D	Canopy disk area, FT^2
S.F.	Snatch factor
S_T	Total canopy cloth area, FT^2
V	Test velocity, FPS

NOMENCLATURE (Cont.)

W	Width of the disk skirt hem between gore center lines, IN.
W_B	Width of the band between gore center lines, IN.

REFERENCES

1. Ludtke, W.P., *A View on the Cause of Parachute Instability*, NSWC/WO TR 83-28.

DISTRIBUTION

	Copies
Commander Naval Air Systems Command Attn: Library	4
AIR-931H (F. Terry Thomasson) Technology Manager Crew Station & Life Support Systems (JP#1-Rm 424)	2
Department of the Navy Washington, DC 20361	
Commander Naval Sea Systems Command Attn: Library	4
Washington, DC 20362	
Commanding Officer Naval Personnel Research and Development Center Attn: Library	2
Washington, DC 20007	
Office of Naval Research Attn: Library	4
Washington, DC 20360	
Office of Naval Research Attn: Fluid Dynamics Branch	2
Structural Mechanics Branch	2
800 N. Quincy St. Arlington, VA 22217	

	Copies
Director Naval Research Laboratory Attn: Code 2027	
Library, Code 2029 (ONRL)	2
Washington, DC 20375	
U.S. Naval Academy Attn: Library	2
Annapolis, MD 21402	
Superintendent U.S. Naval Postgraduate School	2
Attn: Library (Code 0384) Monterey, CA 93940	
Commander Naval Air Development Center Attn: Library	2
Dr. Norman Warner	1
Kenneth Greene	1
William B. Shope	1
David N. DeSimone	1
Louis A. Daulerio	1
Thomas J. Popp	1
Maria C. Hura	1
Warminster, PA 18974	
Commanding Officer Naval Weapons Support Center Attn: Library	2
Mark T. Little	1
Crane, IN 47522	

DISTRIBUTION (Cont.)

	Copies
Commander Naval Ship Research and Development Center Attn: Library Washington, DC 20007	2
Commander Pacific Missile Test Center Attn: Technical Library, Code N0322 Point Mugu, CA 93041	2
Director Marine Corps Development and Education Command Development Center Attn: Library Quantico, VA 22134	2
Marine Corps Liaison Officer U.S. Army Natick Laboratories Natick, MA 01760	2
Commanding General U.S. Army Mobility Equipment Research and Development Center Attn: Technical Document Center Fort Belvoir, VA 22660	2
Commanding General U.S. Army Munitions Command Attn Technical Library Stanley D. Kahn Dover, NJ 07801	2 1
Commanding General U.S. Army Weapons Command Attn: Technical Library Research and Development Directorate Rock Island, IL 61201	2
Commanding General U.S. Army ARDEC Attn: Library Walt Koenig, SMCAR-AET-A Roy W. Kline, SMCAR-AET-A Dover, NJ 07801	2 1 1
Army Research and Development Laboratories Aberdeen Proving Ground Attn: Technical Library, Bldg. 313 Aberdeen, MD 21005	2
Commanding General Edgewood Arsenal Headquarters Attn: Library Aero Research Group Aberdeen Proving Ground Aberdeen, MD 21005	2
Commanding General Harry Diamond Laboratories Attn: Technical Library 2800 Powder Mill Road Adelphi, MD 20783	2

DISTRIBUTION (Cont.)

	Copies
U.S. Army Ballistic Research Laboratories Attn: Technical Library Aberdeen Proving Ground Aberdeen, MD 21005	2
Commanding General U.S. Army Foreign Science and Technoloy Center Attn: Technical Library 220 Seventh Street, NE Federal Building Charlottesville, VA 22312	2
Commanding General U.S. Army Materiel Command Attn: Library Washington, DC 20315	2
Commanding General U.S. Army Test and Evaluation Command Attn: Library Aberdeen Proving Ground Aberdeen, MD 21005	2
Commanding General U.S. Army Combat Developments Command Attn: Library Fort Belvoir, VA 22060	2
Commanding General U.S. Army Combat Developments Command Attn: Technical Library Carlisle Barracks, PA 17013	2
Commanding General U.S. Army Materiel Laboratories Attn: Technical Library Fort Eustis, VA 23604	2
U.S. Army Air Mobility R&D Laboratory Eustis Directorate Attn; Systems and Equipment Division Fort Eustis, VA 23604	2
President U.S. Army Airborne Communications and Electronic Board Fort Bragg, NC 28307	2
Commanding General Frankford Arsenal Attn: Technical Library Bridge and Tacony Streets Philadelphia, PA 19137	2
Commanding General U.S. Missile Command Redstone Scientific Information Center Attn: Library Redstone Arsenal, AL 35809l	2
U.S. Army Natick Laboratories Liaison Office Attn: Library Aeronautical Systems Division Wright Patterson AFB, OH 45433	2

DISTRIBUTION (Cont.)

	Copies
Office of the Chief of Research and Development Department of the Army Attn: Library Washington, DC 20310	2
U.S. Army Advanced Material Concepts Agency Department of the Army Attn: Library Washington, DC 20315	2
Director U.S. Army Mobility R&D Laboratory AMES Research Center Attn: Library Moffett Field, CA 94035	2
Commandant Quartermaster School Airborne Department Attn: Library Fort Lee, VA 23801	2
U.S. Army Standardization Group, UK Attn: Research/General Material Representative Box 65 FPO, NY 09510	2
Commanding Officer McCallan AFB Attn: Library SA-ALC/MMIR McCallan AFB, CA 95652	2
Arnold Engineering Development Center (ARO, Inc.) Attn: Library/Documents Arnold Air Force Sation, TN 37389	2
NASA Lewis Research Center Attn: Library, Mail Stop 60-3 21000 Brookpark Road Cleveland, OH 44135	1
NASA John F. Kennedy Space Center Attn: Library, Code IS-CAS-42B Kennedy Space Center, FL 32899	1
NASA Manned Spacecraft Center Attn: Library, Code BM6 2101 Webster Seabrook Road Houston, TX 77058	1
NASA Marshall Space Flight Center Attn: Library Huntsville, AL 25812	1
NASA Goddard Space Flight Center Wallops Island Flight Facility Attn: Library Mr. Mendle Silbert Mr. Earl B. Jackson, Code 841.2 Mr. Dave Moltedo, Code 841.2 Mr. Anel Flores Wallops Island, VA 23337	2 2 1 1 1
National Aeronautics and Space Administration Attn: Library Headquarters, MTG 400 Maryland Avenue, SW Washington, DC 20456	2

DISTRIBUTION (Cont.)

	Copies
Defense Advanced Research Projects Agency Attn: Technical Library 1400 Wilson Boulevard Arlington, VA 22209	2
Director Defense Research and Engineering Attn: Library (Technical) The Pentagon Washington, DC 20301	2
Director of Defense Research and Engineering Department of Defense Washington, DC 20315	2
Defense Technical Information Center Cameron Station Alexandria, VA 22314	12
Library of Congress Attn: Gift and Exchange Division Washington, DC 20540	4
University of Minnesota Dept. of Aerospace Engineering Attn: Dr. W. L. Garrard Minneapolis, MN 55455	2

	Copies
Sandia National Laboratories Attn: Code 1632	2
Library	2
Dr. Dean Wolf	1
Dr. Carl Peterson	10
R. Kurt Baca	1
Ira T. Holt	1
Donald W. Johnson	1
James W. Purvis	1
Harold E. Widdows	1
Albuquerque, NM 87185	
Applied Physics Laboratory The Johns Hopkins University Attn: Document Librarian Johns Hopkins Road Laurel, MD 20810	2
National Academy of Sciences National Research Council Committee on Undersea Warfare Attn: Library 2101 Constitution Ave., N.W. Washington, DC 20418	2
Sandia Corporation Livermore Laboratory Attn: Technical Reference Library P.O. Box 969 Livermore, CA 9455	2
Lockheed Missiles and Space Co. Attn: Mr. K. French P.O. Box 504 Sunnyvale, CA 94086	1

DISTRIBUTION (Cont.)

	Copies
Rockwell International Corporation Space and Information Systems Div. Attn: Technical Information Center 12214 S. Lakewood Boulevard Downey, CA 90241	2
Pennsylvania State University Applied Research Laboratory Attn: Library P.O. Box 30 State College, PA 16801	2
Honeywell, Incorporated Attn: M. S. Sopczak 600 Second Street N. Hopkins, MN 55343	1
National Bureau of Standards Attn: Library Washington, DC 20234	2
Internal Distribution:	
U13 (C. J. Diehlmann)	1
U13 (W. P. Ludtke)	35
U13 (J. F. McNelia)	1
U13 (D. W. Fiske)	1
U13 (J. Murphy)	1
U13 (M. L. Fender)	1
U13 (R. L. Pense)	1
U13 (M. L. Lama)	1
U43 (J. Rosenberg)	1
E231	2
E232	15
E31 (GIDEP)	1
C72W	1